

ORIGINAL ARTICLE OPEN ACCESS

Food Engineering, Materials Science, and Nanotechnology

Exploring the Potential of Lupin (*Lupinus angustifolius*) Flour-Based Ingredients in Developing High Moisture Meat Analogues

Matias Rodriguez Elhordoy¹ | Aayushi Kadam^{2,3} Daniel Vazquez⁴ Alejandra Medrano¹ Filiz Koksel^{2,3}

¹Departamento de Ciencia y Tecnología de Alimentos, Facultad de Química, Universidad de la República, Montevideo, Uruguay | ²Department of Food and Human Nutritional Sciences, Faculty of Agricultural and Food Sciences, University of Manitoba, Winnipeg, Manitoba, Canada | ³Richardson Centre for Food Technology and Research, University of Manitoba, Winnipeg, Manitoba, Canada | ⁴Instituto Nacional de Investigación Agropecuaria (INIA), Área Agroalimentos, Estación Experimental INIA La Estanzuela, Colonia, Uruguay

Correspondence: Filiz Koksel (filiz.koksel@umanitoba.ca)

Received: 20 March 2025 | Revised: 12 June 2025 | Accepted: 26 June 2025

Funding: The financial support for this project was provided by the Natural Sciences and Engineering Research Council (NSERC) Canada, Discovery Grants program for F. Koksel. Infrastructural support was provided by the Canada Foundation for Innovation (CFI) JELF program. Additional financial support was received from the Agencia Nacional de Investigación e Innovación (ANII) MR through scholarships POS_NAC_2022_1_174183 and MOV_CA_2021_1_171688; Programa de Desarrollo de las Ciencias Básicas (PEDECIBA); and Comisión Sectorial de Investigación Científica through Project 22420230100104UD

Keywords: extrusion cooking | lupin protein | meat alternatives | protein digestibility | soy protein | sustainable food systems

ABSTRACT

The rising demand for sustainably and ethically produced alternatives to animal protein-rich foods has driven interest in plant-based meat analogues. This study evaluated the potential of lupin flour (LF), protein isolate (LPI), and their blends with soy protein isolate (SPI) to produce high-moisture meat analogues (HMMAs) through extrusion cooking. Six SPI-LF-LPI blends, with protein contents ranging from 64.5% to 80.5%, were extruded under three feed moisture contents (FMC) of 60%, 65%, and 70%. Increasing LF content affected the textural attributes of the HMMAs, reducing their hardness, chewiness, and gumminess. The peak force to cut the HMMAs in longitudinal and transverse directions ranged from 3.3 to 10 N, with the softest textures observed for blends containing relatively higher LF and LPI and at the higher FMC level of 70%. In vitro protein digestibility of the HMMAs improved with increasing FMC, reaching a maximum proteolysis degree of 51.5% for the blend containing 55% SPI and 45% LF produced at 70% FMC. Although extrusion reduced the antioxidant capacity of the HMMAs compared to their raw counterparts, the antioxidant capacity of the HMMAs increased as the FMC level increased. These findings highlight the feasibility of using lupin ingredients to produce nutritionally rich and texturally appealing plant-based meat analogues when extrusion conditions are fine-tuned.

Matias Rodriguez Elhordoy and Aayushi Kadam contributed equally to this work.

This is an open access article under the terms of the Creative Commons Attribution-NonCommercial-NoDerivs License, which permits use and distribution in any medium, provided the original work is properly cited, the use is non-commercial and no modifications or adaptations are made.

© 2025 The Author(s). Journal of Food Science published by Wiley Periodicals LLC on behalf of Institute of Food Technologists.

1 | Introduction

The consumption of plant-based meat alternatives is increasing due to rising public awareness of health concerns, ethical considerations, and environmental impacts associated with meat consumption (Ramos-Diaz et al. 2023). Efforts to develop sustainable foods from plant-based ingredients, like those from grains, align with the United Nations Sustainable Development Goals (UNDP n.d.). However, reliance on feed grains that are well suited for a wide range of plant-based foods but not grown locally presents similar environmental challenges. This highlights the need for locally sourced protein alternatives with lower environmental impact to enhance sustainability and food system resilience (Ramos-Diaz et al. 2023; Rapinski et al. 2023).

Lupin seeds have gained significant attention as an alternative to conventional protein sources due to their rich nutritional profile and sustainability. They are high in protein, containing approximately 40-45% protein on a dry weight basis (db), an excellent source of dietary fiber, and a valuable source of lipids, containing 6-7% unsaturated fatty acids such as oleic, linoleic, and linolenic acids, along with essential vitamins (thiamine, riboflavin, niacin, and carotenoids) and minerals (Ca, K, Na, Mg, Fe, Zn, and Mn) (Devkota et al. 2023; Estivi et al. 2023). Moreover, lupine seeds are rich in bioactive compounds, including carotenoids, tocopherols, and phenolic compounds, which are mainly present in their free form (~90%), followed by the soluble conjugated and insoluble bound forms, which contribute to their antioxidant properties (Estivi et al. 2023; Lemus-Conejo et al. 2023; Villarino et al. 2016). These compounds help stabilize free radicals, preventing oxidative stress and damage to essential biomolecules such as membranes, lipids, proteins, and DNA, which are linked to the onset of various chronic diseases (Estivi et al. 2023), and enhance the overall nutritional value of lupin seeds. However, the bioavailability and efficacy of these bioactive compounds depend not only on their initial content in foods but also on their stability and transformation throughout digestion. Phenolic compounds, in particular, undergo metabolic modifications in the gastrointestinal tract, which can influence their antioxidant activity and overall functionality (Fernández-Fernández et al. 2021; Fernández-Fernández et al. 2022). Therefore, understanding the behavior of these compounds after digestion is essential for evaluating their true biological potential.

Among the various lupin species, narrow-leafed blue lupin (*Lupinus angustifolius*) is gaining attention for its high protein content, low level of antinutritional factors, and health benefits. These benefits include positive effects on diseases such as type 2 diabetes, dyslipidemias, hypertension, neurodegenerative diseases, and cancer, owing to its bioactive compounds including phenolic compounds, and protein hydrolysates (Cortés-Avendaño et al. 2020; Lemus-Conejo et al. 2023; Pasarin et al. 2023). This species is increasingly being explored for its potential in plant-based food innovations, offering a nutritious and sustainable ingredient with health-promoting properties (Pasarin et al. 2023).

A nutritional profile comparable to soybeans in terms of protein and fiber content (Beyer et al. 2015; Sujak et al. 2006), makes lupin seeds a versatile ingredient for a variety of food products, such as cakes, pancakes, biscuits, pasta, and bread (Dervas et al. 1999). Lupin-based dairy substitutes, such as milk and yogurt, are also gaining popularity in response to the growing demand for plant-based alternatives to dairy products (Hickisch et al. 2016; Hickisch, Bindl, et al. 2016). Beyond its nutritional properties, lupin contributes to environmental sustainability by fixing atmospheric nitrogen, reducing greenhouse gas emissions, and improving soil health, thus supporting sustainable agricultural practices (Barton et al. 2014; Ferchichi et al. 2021; Roman et al. 2023; Seregina et al. 2024).

High-moisture extrusion cooking is a promising technique for creating plant-based meat analogues with fibrous texture and appealing sensory properties, using various plant protein sources, including lupin (Ramos-Diaz et al. 2023). Despite lupin's promising nutritional profile and sustainability, lupin flour (LF) and lupin protein isolate (LPI) remain underexplored in highmoisture meat analogue (HMMA) production, especially in combination with other plant proteins like soy protein isolate (SPI). To date, SPI remains the most widely studied and utilized plant protein ingredient for the production of plant-based meat analogues, owing to its high protein content, excellent gelation and fibrous structure-forming properties, relatively balanced amino acid profile, and neutral flavor and color (Dekkers et al. 2018; Schreuders et al. 2019; Zhang et al. 2020). Although the industrial process to obtain SPI involves significant protein denaturation, potentially altering its physicochemical characteristics, SPI-based formulations have consistently demonstrated superior fibrous structure formation under high-shear extrusion conditions (Osen et al. 2014). Given this well-established functionality, SPI was selected as the main structural base in this

A previous study on lupin-based HMMAs utilized LPI-LF blends, highlighting lupin's potential for HMMA applications but reaching LF concentrations only up to 30% in the formula (Ramos-Diaz et al. 2023). In this study, we explored a much wider LF concentration (up to 45%) and examined how extrusion conditions impacted both the textural and nutritional attributes of HMMAs made from blends of SPI, LF, and LPI. Using flours instead of highly processed protein isolates or concentrates offers a more practical and sustainable approach to manufacturing meat analogues by reducing processing requirements and preserving more of the ingredient's natural components. The findings provide critical insights into designing lupin-based HMMAs with enhanced textural, functional, and nutritional quality. Given that lupins are naturally rich in antioxidants and bioactive compounds, they represent a valuable ingredient in the formulation of functional foods. Incorporating lupin-derived ingredients supports the development of scalable plant-based meat alternatives by not only improving structural and sensory attributes but also enhancing oxidative stability and shelf life due to their antioxidant bioactive compounds. Furthermore, the presence of bioaccessible antioxidant compounds may contribute to the prevention of oxidative stress-related diseases, aligning with emerging consumer

trends that favor healthier, functional, and sustainable food products.

2 | Materials and Methods

2.1 | Materials

SPI (SUPRO EX45) was procured from Azelis Canada Inc. (Brampton, ON, Canada). *Lupinus angustifolius* (cultivar Lila Baer) beans were received from Juan Pablo Viera (Colonia, Colonia, Uruguay). The unshelled full-fat seeds were milled at Molino Guido (Santiago Vázquez, Montevideo, Uruguay) using a Miag HN roller mill (Miag, Braunschweig, Germany) to obtain LF with a particle size less than 1 mm. Part of this flour was used to extract LPI as described below. The remaining flour was milled using a centrifugal mill (Retsch ZM200, Retsch GmbH, Haan, Germany) at 6,000 rpm, with a 500 μ m sieve to further reduce the particle size.

2.2 | Preparation of the LPI

LPI was extracted from the LF according to Berghout et al. (2014). Briefly, LF was suspended in distilled water at a 1:20 (w/v) ratio and the pH was adjusted to 9.0 \pm 0.5 using 1 M NaOH. The suspension was stirred using a magnetic stirrer at 500 rpm for 2 h at room temperature and then stored at 4°C for 48 h. After centrifugation (Sorvall RC-6 plus, Thermo Fisher Scientific, NC, USA) at $1050\times g$ for 15 min at $20^{\circ}C$, the supernatant was collected and acidified to pH 4.5 \pm 0.5 using 1 M HCl and stirred at room temperature for 1 h. To recover the protein, the solution was centrifuged at $13500\times g$ at $25^{\circ}C$ for 20 min. The protein-rich pellet was dissolved in water, and the pH was adjusted to 7.0 \pm 0.3. The solution was then frozen at -15°C and freeze-dried. The freeze-dried material, i.e., the LPI, was stored at 4°C in vacuum bags until use. The protein isolate yield (%) was determined according to Cháirez-Jiménez et al. (2023) following equation (1):

Protein Yield (%) =
$$\left(\frac{\text{Protein content in LPI} \times \text{Yield of LPI}}{\text{Protein content in LF}}\right)$$
×100 (1)

2.3 | Proximate Composition

Proximate analysis of raw materials was carried out in triplicate following the AACC International (2010) methods for moisture (method 44-19.01), ash (method 08-01.01), and crude protein (method 46-30.01). Fat and total dietary fiber were measured according to the AOAC (2005) standard methods 2003.06 and 985.29, respectively. Total carbohydrate content was calculated by the difference between the total dry weight and the weights of ash, crude protein, and fat on a db.

2.4 | Particle Size Distribution

Particle size distribution of SPI, LF, and LPI was determined using a laser diffraction particle size analyzer (Mastersizer 3000,

Malvern Instruments Ltd., Malvern, UK). Volume mean diameter D[4,3] was determined along with the particle size thresholds below 10, 50, and 90% volume of the particle size, denoted as d(0.1), d(0.5), and d(0.9), respectively.

2.5 | Preparation of Blends for Extrusion

Six different blends of SPI, LF, and LPI were prepared as presented in Table 1. The raw materials were weighed and mixed in a blender (LBB Bohle LM40, Bohle Maschinen und Verfahren GmbH, Germany) for 20 min at 50 rpm.

2.6 | Pasting Properties

Pasting properties of the raw material blends were measured using a rheometer (MCR 92, Anton Paar, Graz, Australia), with a measuring cup (C-CC27/T200/SS) and stirrer (ST24-2D/2 V/2V-30/109) (Patil et al. 2020). Briefly, each blend (2.5 g, 14% moisture basis) was mixed with 20 mL of deionized water to prepare a slurry. The viscosity of the slurry was measured during the following conditions: holding the slurry at 50°C for 60 s with a pre-stirring stage of 30 s at 960 rpm, then heating it to 95°C at a rate of 3.5°C/min, holding it at 95°C for 5 min, and then cooling it down to 50°C at a rate of 3.5°C/min. Unless otherwise stated, the test speed was 160 rpm. Duplicate measurements were performed for each blend.

2.7 | High Moisture Extrusion Cooking

Extrusion was performed in triplicate using a lab-scale, corotating, twin-screw extruder (MPF19, APV Baker Ltd., Peterborough, UK). The extruder, with a screw length-to-diameter ratio of 25:1, was configured as reported by Koksel and Masatcioglu (2018). The feed rate (0.5 kg/h db), the screw speed (200 rpm), and the barrel and die temperature profiles were kept constant. The barrel with 4 different temperature zones from the feeder to the die was set according to Guillermic et al. (2023) as 60-80-110-120°C. For the long cooling die (inside dimensions: 300 \times 50×5 mm), the temperature was set at 80° C close to the barrel and 50°C at the exit. Three different FMCs of 60%, 65%, and 70% (wet basis) were used for each of the 6 blend formulations, and the reported HMMA moisture levels are based on these feed moisture content values, not on post-extrusion measurements. Die pressure (kPa) and torque (%) values were recorded in quadruplicates during extrudate collection. Specific mechanical energy input, SME (Wh/kg), was calculated according to Luo and Koksel (2020). Long strips of HMMAs collected were stored in zipped plastic bags at −25°C.

2.8 | Textural Properties of the HMMAs

Textural properties of the HMMAs were analyzed using a texture analyzer (TA-XT-plus, Stable Micro Systems, Godalming, UK). Cutting strength tests were performed in the longitudinal (parallel to the extrudate flow direction inside the die) and transverse (perpendicular to the extrudate flow direction inside the die) directions following the method of Ghanghas et al. (2024). Briefly,

TABLE 1 Blends of soy protein isolate (SPI) with lupin flour (LF) and lupin protein isolate (LPI).

Formulation	SPI (%)	LF (%)	LPI (%)	Protein content (% db)*
Blend 1	85	15	0	80.52
Blend 2	75	25	0	75.18
Blend 3	65	35	0	69.84
Blend 4	55	45	0	64.50
Blend 5	55	40	5	66.91
Blend 6	55	35	10	69.32

^{*}Protein content was calculated based on the protein content of the raw materials.

the HMMAs were thawed, brought to room temperature, and then cut into square pieces of 20 mm \times 20 mm (thickness: 5 mm). HMMA pieces were then cut using a craft knife accessory (A/ECB blade probe) and a load cell of 5 kg. The following settings were used: pre-test speed of 1 mm/s, test speed of 2 mm/s, post-test speed of 10 mm/s, cutting distance of 75% of the HMMA thickness. The maximum cutting force was obtained from the force vs. time graph.

To evaluate the anisotropy of the HMMA structure formed during extrusion, the degree of texturization (DT) was calculated following equation (2) as described by Ghanghas et al. (2024), where F_T is the cutting force in the transverse direction and F_L is the cutting force in the longitudinal direction.

$$\mathbf{DT} = \frac{\mathbf{F}_{\mathrm{T}}}{\mathbf{F}_{\mathrm{r}}} \tag{2}$$

Texture profile analysis (TPA) was performed according to Singh et al. (2025). A cylindrical probe (38 mm diameter) with a load cell of 30 kg was used for the test at the following settings: strain of 50%, pre-test speed of 1 mm/s, test speed of 2 mm/s, post-test-speed of 10 mm/s, and trigger force of 0.049 N. From the force vs. time graph of two compression-decompression cycles of the 20 mm \times 20 mm HMMA pieces, the following attributes were determined: hardness, resilience, springiness, and chewiness (Singh et al. 2024).

2.9 | Color Analysis

The color characteristics of the raw material blends and the HMMAs were measured using a Minolta CM-3500d spectrophotometer (Osaka, Japan). Before measurements, the HMMAs were thawed and brought to room temperature. Six measurements of L* (lightness), a* (greenness-redness), and b* (blueness-yellowness) were performed at random surface locations of the HMMAs. The total color difference (ΔE) between the raw blends and their corresponding extrudates was calculated using equation (3):

$$\Delta E = \sqrt{(\mathbf{L_H}^* - \mathbf{L_R}^*)^2 + (\mathbf{a_H}^* - \mathbf{a_R}^*) + (\mathbf{b_H}^* - \mathbf{b_R}^*)}$$
 (3)

Where L_H^* , a_H^* and b_H^* represent the parameters lightness, greenness-redness, and blueness-yellowness, respectively, for HMMAs. L_R^* , a_R^* , and b_R^* correspond to the parameters of the raw material blends.

2.10 | Macrostructure of HMMAs

The visual appearance and qualitative macrostructure of the HMMA were documented through digital photographs taken immediately after extrusion (iPhone 11, Apple Inc., Cupertino, CA, USA) equipped with a 12-megapixel wide-angle (f/1.8 aperture) and an ultra-wide-angle (f/2.4 aperture) lens. For macroscopic visualization, HMMA strips were longitudinally cut open to reveal their internal fibrous structure.

2.11 | In vitro Protein Digestibility

Blends containing SPI and LF, i.e., blends 1–4, along with their respective HMMAs at FMC levels of 60% and 70% (moisture extremes), were selected for digestibility analysis. The inclusion of LPI did not result in substantial differences in the texture and color of the HMMAs compared to formulations containing only LF. Given the minimal impact of LPI on product quality and the greater economic feasibility of LF, further analysis was focused on SPI-LF-based HMMAs. Additionally, to understand the influence of extremes of FMC studied on the functional properties of the HMMAs, the lowest (60%) and highest (70%) FMCs were selected.

In vitro gastrointestinal digestion was performed following the standardized INFOGEST protocol, which involves successive oral, gastric, and intestinal digestive phases (Brodkorb et al. 2019). For the oral digestive phase, 2.5 g of each sample was weighed and mixed with simulated salivary fluid (pH 7, electrolytes, α amylase) and incubated at 37°C for 5 min with constant stirring. Subsequently, in the gastric digestive phase, simulated gastric fluid (pH 3, electrolytes, pepsin, gastric lipase) was added to this mixture and incubated for 2 h with constant stirring at 37°C. The intestinal digestive phase consisted of adding simulated intestinal fluid (pH 7, electrolytes, pancreatin, bile, NaHCO₃) and incubating for an additional 2 h at 37°C. After digestion, the samples were cooled in an ice bath for 10 min, centrifuged (10 min, $1050 \times g$, 25° C), and separated into two fractions: the bio-accessible fraction (supernatant) and the colonic fraction (insoluble residue, pellet) (Fernández-Fernández et al. 2021). The samples were then stored at -20° C until further analysis.

The degree of proteolysis was determined by quantifying the free amino groups that react with o-phthalaldehyde (OPA), following the methodology described by Rodríguez Arzuaga et al. (2024). About 200 μ L of each bio-accessible fraction was mixed with OPA reagent, and the absorbance of the mixture was measured

at 340 nm using a spectrophotometer (Varioskan Lux, Thermo Scientific, MA, USA).

To determine total free amino acid content, acid hydrolysis was performed by adding 5 mL of 6 N HCl to 200 mg of ground HMMA samples and raw materials, followed by heating at 110° C for 24 h. The hydrolysate was filtered and stored at -20°C until further analysis. The total free amino groups in the hydrolysate were quantified using the OPA method as described above.

The degree of proteolysis was calculated using equation (4):

Degree of proteolysis

$$= \left(\frac{Concentration of free \alpha - amino groups in the digested sample}{Concentration of total \alpha - amino groups in the acid hydrolysed sample}\right) \times 100$$
(4)

2.12 | Antioxidant Capacity

The antioxidant capacity of the raw blends and their extrudates extracted with 50% dimethyl sulfoxide (6.7 w/v) was measured using ABTS'+ (scavenging of 2,2'-azino-bis(3-ethylbenzothiazoline-6-sulfonic acid)) and ORAC-FL (oxygen radical absorption capacity) methods, as described by Olt et al. (2023) and Báez et al. (2021), respectively. Results were expressed as μ M Trolox Equivalents (TE) per g of sample. Additionally, the antioxidant capacity of the digested fractions was measured to evaluate their bioaccessibility (Fernández-Fernández et al. 2021).

2.13 | Statistical Analysis

All analyses were performed at least in triplicate, except for pasting properties, which were performed in duplicate. Data was analyzed using one-way ANOVA and Tukey's test to determine significant differences at a level of p < 0.05 using InfoStat v 2020 software (Universidad Nacional de Córdoba, Cordoba, Argentina).

3 | Results and Discussion

3.1 | Proximate Composition of the Raw Materials

The proximate analyses of SPI, LF, and LPI showed that both SPI and LPI had high protein contents of 88.5% and 85.2%, respectively (Table 2). LF had a relatively lower protein content of 35.1%, but a very high dietary fiber content of 42.3%. This elevated fiber level can be beneficial to enhance nutritional profile and texture of HMMAs. Dietary fibers influence the texturization of meat analogs by modulating phase separation and water absorption of HMMAs (van der Sman and van der Goot 2023). Insoluble fibers, such as cellulose, contribute to a tougher texture in meat analogs and may lead to macroscopic phase separation, while soluble fibers, such as pectin, enhance water retention and soften the texture, potentially resulting in a mushier consistency (Schreuders et al. 2022). LF also had a relatively high fat content (7.4%) compared to SPI (3.1%) and LPI (3.7%), which may improve the flavor and mouthfeel of the HMMAs (Zhang et al. 2024).

The ash content, indicative of mineral presence, was comparable across all the raw materials. Additionally, LF's high carbohydrate content (11.7) may influence the caloric value of the end product, while the lower carbohydrate levels in SPI (4.5%) and LPI (1.4%) are beneficial for low-carbohydrate formulations.

The results of the proximate composition analyses are consistent with Bähr et al. (2014) who reported protein content ranging from 38.8% to 44.2%, dietary fiber from 36.7% to 40.01%, lipid from 6.8% to 9.8%, total carbohydrates from 6.1% to 8.0% and ash from 3.72% to 4.17% in various cultivars of *Lupinus angustifolius*. Similarly, Lemus-Conejo et al. (2023) reported 33.9% of protein, 37.5 - 40.2% total dietary fiber, and 6–7% fat in *L. angustifolius*.

During the extraction of lupin protein, a yield of 23.05% was achieved, with a crude protein content of 85.2% (db) (Table 2). Based on these values and the initial protein content of the LF, the protein recovery yield was calculated to be approximately 56%, indicating that slightly more than half of the total protein originally present in the LF was successfully extracted. This finding aligns with Albe-Slabi et al. (2022) who reported lupin protein extraction yields ranging from 41% to 43% across a pH range of 7–10. Additionally, Lqari et al. (2002) reported an 88.9% protein content in LPIs produced by alkaline extraction at pH 10.5.

3.2 | Particle Size Distribution of the Raw Materials

The particle size distributions of the raw materials are illustrated in Figure 1. Among the raw materials used, LF exhibited the largest particle sizes across all measured percentiles, with d(0.1) at 78.1 $\mu m,\ d(0.5)$ at 489.3 $\mu m,\ and\ d(0.9)$ at 957.7 $\mu m.$ LF had a relatively wider distribution of particle sizes, suggesting a more heterogeneous mixture of fine and coarse particles, when compared to SPI.

LPI displayed intermediate particle sizes, with d(0.1), d(0.5), and d(0.9) recorded at 26.7 μ m, 125.5 μ m, and 199.5 μ m, respectively. SPI showed the smallest particle sizes, with d(0.1) at 14.2 μ m, d(0.5) at 52.6 μ m, and d(0.9) at 66.3 μ m. The narrowest particle size distribution of the SPI indicated a high degree of refinement and homogeneity. The average volume diameter, D[4,3], which represents a volume-weighted mean particle size, further supports these observations. SPI had the lowest D[4,3] value at 66.3 μ m, indicating the finest particles. LPI had a D[4,3] of 199.5 μ m, while LF had the highest D[4,3] at 515.3 μ m, highlighting the significant differences in particle size distribution among the raw materials.

Particle size distribution can influence the techno-functional properties of raw materials. For example, smaller particles, like those in SPI, can enhance their solubility in water (Yang et al. 2018; Zhang et al. 2020). Conversely, the broader size distribution of the LF particles may affect LF's hydration properties (Bressiani et al. 2021).

3.3 | Pasting Properties

Pasting properties were evaluated by gradually heating the hydrated blends up to 95°C to characterize the gelatinization,

TABLE 2 | Proximate composition of the raw material blends.

Composition (% db)	SPI	LF	LPI
Protein	88.5 ± 1.6	35.1 ± 0.3	85.2 ± 1.6
Fat	3.1 ± 0.1	7.4 ± 0.2	3.7 ± 0.0
Ash	3.9 ± 0.0	3.5 ± 0.1	3.3 ± 0.0
Dietary fiber	ND	42.3 ± 0.7	6.4 ± 0.3
Non-dietary fiber carbohydrates	4.5	11.7	1.4

Note: Data is expressed as mean \pm standard deviation (n = 3).

Abbreviations: SPI, soy protein isolate; LF, lupin flour; LPI, lupin protein isolate; ND, not detectable.

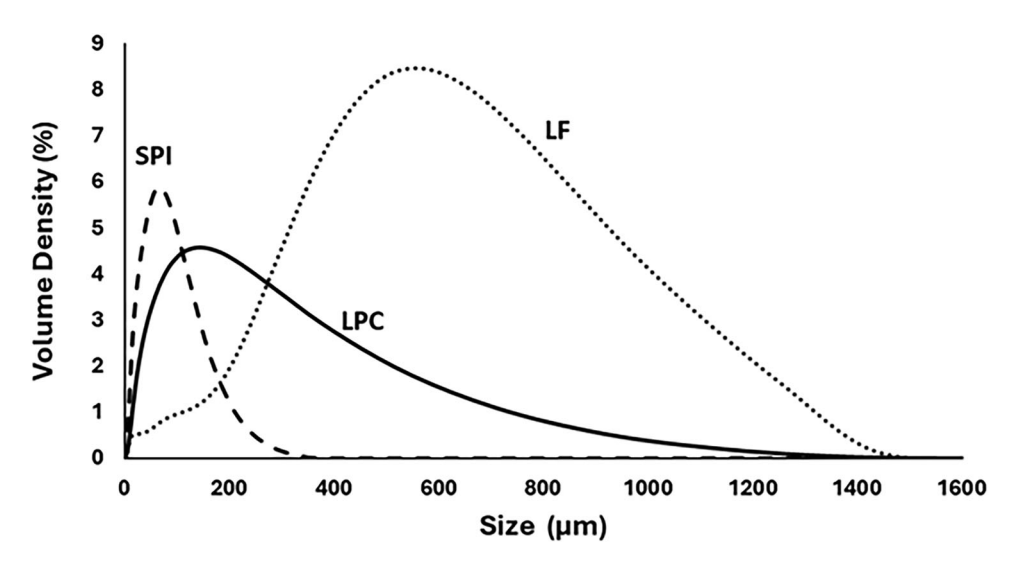


FIGURE 1 | Particle size distribution of the raw materials. SPI: soy protein isolate, LPI: lupin protein isolate, LF: lupin flour.

TABLE 3 | Pasting properties of the raw blends.

Formulation	Peak viscosity (cP)	Final viscosity (cP)
Blend 1 (85SPI:15LF)	391.9 ± 4.9^{a}	178.0 ± 20.0^{b}
Blend 2 (75SPI:25LF)	239.6 ± 11.2^{b}	195.0 ± 12.0^{a}
Blend 3 (65SPI:35LF)	$135.8 \pm 1.7^{\circ}$	191.3 ± 3.1^{a}
Blend 4 (55SPI:45LF)	63.0 ± 3.2^{d}	131.9 ± 21.9^{cd}
Blend 5 (55SPI:40LF:5LPI)	$70.7 \pm 0.6^{\rm e}$	139.4 ± 2.8^{d}
Blend 6 (55SPI:35LF:10LPI)	$83.9 \pm 2.0^{\rm f}$	$145.2 \pm 1.5^{\circ}$

Note: Data is presented as mean \pm standard deviation (n = 2). In each column, values with different letters are significantly different (p < 0.05). Abbreviations: SPI, soy protein isolate; LF, lupin flour; LPI, lupin protein isolate.

protein hydration, and fiber-water interactions (Figure S1). While this temperature range does not replicate the high-temperature conditions of the extrusion cooking process, it is commonly used to assess functional transitions in plant-based matrices prior to extrusion. Standard RVA profiles have been proposed as a simple tool for screening ingredients for the extrusion cooking process (Osen et al. 2014).

Pasting properties, namely peak and final viscosities, of the raw blends are summarized in Table 3. Peak viscosity decreased as the proportion of LF increased in the blends. Blend 1, which had the highest protein content (80.52%), exhibited the highest peak viscosity (391.9 cP). In contrast, blend 4, with the lowest protein content (64.50% protein), showed the lowest peak viscosity at 63.03 cP. The observed reduction in viscosity with increasing LF content can be attributed to the lower protein content of LF compared to SPI. Lower protein levels generally lead to a reduction in viscosity due to reduced protein-protein interactions and gel strength, especially during the cooling stage (Dikeman and Fahey Jr. 2006; Zhang and Liu 2017). Additionally, both soluble

and insoluble fibers of LF can limit protein gelation—insoluble fibers physically entrap proteins within cellular matrices, while soluble fibers compete for water and alter protein interactions (Badjona et al. 2025). In line with this, blend 6, despite having a protein content similar to blend 3, exhibited a relatively lower peak viscosity, which can be attributed to its higher fiber content (Table 2) compared to blend 3 (Dikeman and Fahey Jr. 2006; Zheng et al. 2021).

Final viscosity reflects a slurry's ability to form a viscous paste or gel after cooking and cooling. Blends 1 and 2, with higher SPI content, had final viscosities lower than their peak viscosities, indicating shear-thinning behavior. In contrast, blends with higher LF (blends 3 and 4) and LPI (blends 5 and 6) displayed final viscosities higher than their peak values. This suggests that blends 3-6, which started with lower viscosities, experienced a viscosity increase over the course of the test, likely due to their relatively higher fiber content compared to blends 1 and 2. Fibers, with their strong water-binding capacity, reduce the availability of free water after cooling, leading to increased viscosity (Zheng et al. 2021). Mazumder et al. (2021) observed a similar trend in the pasting properties of different lupin cultivars. These align with the fact that LF contains minimal starch, and therefore its RVA viscosity profile primarily depends on the hydration properties of lupin proteins and fibers. Overall, these results underscore the strong correlation between raw material composition and apparent viscosity, emphasizing the critical role of blend formulation in determining rheological properties during extrusion.

Blends 1 and 2, with higher SPI content, exhibited higher peak viscosities and lower breakdown values during Rapid Visco Analyzer (RVA) analysis. This behavior may have contributed to the denser, firmer structures observed in these samples postextrusion, as indicated by their higher hardness, gumminess, and chewiness values. The increased peak viscosity suggests a stronger gel-forming ability and greater resistance to shear and thermal degradation, which are essential for developing a cohesive and fibrous texture during high-moisture extrusion. Similarly, Hwang et al. (2024) found that isolated mung bean protein contributed to an increase in viscosity and enhanced fibrousness in extruded products. In addition, Plattner et al. (2024) reported a similar trend where a higher viscosity was correlated with better texturization in pea protein isolate-based HMMAs. Such correlations emphasize the importance of selecting protein ingredients with favorable pasting properties to optimize the technological and sensory qualities of plant-based meat analogues.

3.4 | Effects of Blend Formulation and FMC on Extrusion Parameters

The torque, die pressure, and SME values during extrusion as a function of protein blend composition and FMC are presented in Table 4. Torque, die pressure, and SME significantly (p < 0.05) decreased with an increase in FMC for all blends. The lower die pressure at higher FMC can be attributed to the lubrication effect of water, which reduces the viscosity of the melt, consequently decreasing the die pressure during extrusion processing (Chen et al. 2010; Palanisamy et al. 2019; Saldanha do Carmo et al. 2021).

Overall, blends 1 and 2 exhibited significantly (p < 0.05) higher torque values at 60% FMC compared to the other blends at the same moisture content. The overall higher torque values observed for these blends can be attributed to their lower lipid content (Kendler et al. 2021) compared to blends 3–6.

SME input values were highest at 60% FMC and decreased with increasing FMC, following the same trend as torque and die pressure. This is likely due to the lower viscosity and improved flow properties imparted by the higher FMC. Likewise, Guillermic et al. (2023) and Singh et al. (2024) demonstrated a reduction in torque, die pressure, and SME values with increasing FMC for soy-wheat protein and soy-sunflower meal HMMAs, respectively. The decrease in SME values with increasing LF content may also be attributed to the larger particle size of LF. A similar trend of reduced SME with increasing particle size was reported for soybean meal (Singh and Koksel 2021).

3.5 | Textural Properties of HMMAs

The results of the peak longitudinal and transverse force to cut the HMMAs are presented in Figure 2a and b. The peak cutting force, in both directions, of all the HMMAs produced decreased significantly (p < 0.05) with increasing FMC, consistent with the findings for soy, hemp, and lupin protein-based HMMAs (Lin et al. 2000; Palanisamy et al. 2019; Zahari et al. 2020). This decline can be attributed to the higher water content diluting the total protein concentration in the melt, reducing the likelihood of protein cross-linking during extrusion, and leading to softer textures (Lin et al. 2000). Additionally, higher FMC decreases shear and friction in the extruder, further contributing to softer textures (Singh et al. 2024). These findings emphasize the critical interplay between processing conditions and protein interactions in determining the cutting force and texture properties of these HMMAs.

Blend formulation also influenced the peak cutting force, revealing notable differences in the textural properties of the HMMAs. HMMAs produced from blends with higher SPI content (blends 1 and 2) exhibited higher cutting forces, indicating a firmer texture, with the maximum cutting forces observed at relatively lower FMCs of 60% and 65%. This suggests that higher SPI content promotes the formation of a denser and stronger protein network, contributing to firmer textures, aligning with previous findings that high protein content enhances network formation and firmness (Luo and Koksel 2020; Wang et al. 2017; Yang et al. 2020). Conversely, HMMAs from blends with higher LF and LPI content (blends 4-6) exhibited lower cutting forces. Elevated concentrations of LF and LPI in the blends decreased the overall protein content of the blends (Table 1), reducing the likelihood of protein cross-linking during extrusion and resulting in softer structures. Similar trends have been reported in studies on HMMAs made from faba bean protein (Kantanen et al. 2022) and soy-sunflower meal blends (Singh et al. 2024). Blend 6 demonstrated the lowest cutting force in both directions overall, particularly at 70% FMC.

Overall, the peak cutting force in the transverse direction was higher than that in the longitudinal direction, suggesting that the structure predominantly formed along the longitudinal axis.

17503841, 2025, 7, Downloaded from https://ift.onlinelibrary.wiley.com/doi/10.1111/1750-3841,70407 by Anit-Agencia Nacional De, Wiley Online Library on [15.09/2025]. See the Terms and Conditions and-conditions) on Wiley Online Library for rules of use; OA articles are governed by the applicable Creative Commons License

TABLE 4 | Effect of blend formulations and feed moisture content (FMC) on extrusion parameters and texture profile attributes.

	FMC %	Torque (%) D	FMC % Torque (%) Die pressure (kPa) SME (Wh/kg)	SME (Wh/kg)	Hardness (N)	Springiness	Gumminess (N)	Chewiness (N)
Blend 1	09	$12.0\pm0.0^{\rm a}$	$546.7 \pm 51.6^{\text{f}}$	82.8 ± 0.0^{b}	190.3 ± 10.0^{b}	$1.0 \pm 0.1^{\mathrm{a}}$	158.0 ± 10.4^{b}	154.8 ± 12.7^{a}
(85SPI:15LF)	65	$10.1\pm0.3^{\rm d}$	$335.7 \pm 49.7^{\rm h}$	$60.5 \pm 1.7^{\rm e}$	$173.1\pm8.2^{\rm cd}$	$0.9\pm0.0^{\rm a-f}$	150.6 ± 7.7^{b}	$141.7 \pm 9.8^{\rm b}$
	70	$8.8 \pm 0.4^{\mathrm{f}}$	173.3 ± 45.8^{i}	$45.1\pm2.1~\mathrm{g.h}$	$89.9 \pm 4.8^{\circ}$	$1.0 \pm 0.0^{ m abcd}$	76.9 ± 3.9^{i}	73.4 ± 3.5 ^{gh}
Blend 2	09	$12.0\pm0.0^{\rm a}$	986.7 ± 35.2 a	$92.3\pm0.0\mathrm{^a}$	208.1 ± 7.9^{a}	$1.0\pm0.0^{\mathrm{a-e}}$	167.0 ± 7.8^{a}	158.8 ± 9.7^{a}
(75SPI:25LF)	65	$10.1\pm0.4^{\rm d}$	$626.7 \pm 7.3^{d,e}$	$68.0 \pm 2.4^{\circ}$	$179.6\pm4.1^{\rm c}$	$0.9\pm0.0^{\text{b-f}}$	153.0 ± 4.0^{b}	141.9 ± 5.2^{b}
	70	$9.0 \pm 0.0^{\mathrm{f}}$	400.0 ± 0.0 g	$51.6\pm0.0^{\rm f}$	$131.8\pm4.4^{\rm g}$	$0.9\pm0.0^{\text{b-f}}$	$110.8 \pm 4.0^{\rm h}$	$102.5 \pm 4.0^{\circ}$
Blend 3	09	$11.0\pm0.0^{\rm b}$	900.0 ± 53.5 b	$82.0 \pm 0.0^{\mathrm{b}}$	$170.5\pm7.7^{\rm d}$	$1.0\pm0.1^{\rm abcd}$	130.0 ± 5.9^{cd}	$124.3 \pm 7.2^{\circ}$
(65SPI:35LF)	65	$10.0\pm0.0^{\rm d}$	$612.3 \pm 64.0^{\circ}$	$64.9 \pm 0.0^{ m d}$	$151.4 \pm 2.8^{\rm ef}$	$0.9\pm0.0^{ m ef}$	$125.1 \pm 2.4^{\rm de}$	113.2 ± 4.0^{d}
	70	8.2 ± 0.4^{g}	413.3 ± 35.2^{g}	$45.5\pm2.3~\mathrm{g,h}$	104.6 ± 3.7^{i}	$0.9\pm0.0^{ m ef}$	85.4 ± 3.4^{i}	$77.2\pm4.6^{\rm g}$
Blend 4	09	10.9 ± 0.3^{b}	$826.7 \pm 45.8^{\circ}$	82.7 ± 5.9^{b}	$158.3 \pm 13.4^{\rm ef}$	$1.0\pm0.1^{\rm ab}$	$116.3\pm10.1^{\mathrm{fgh}}$	$112.9\pm9.6^{\rm d}$
(55SPI:45LF)	65	$10.0\pm0.0^{\rm d}$	$613.3 \pm 35.2^{\circ}$	$67.1 \pm 0.0^{\text{c,d}}$	$152.8 \pm 4.2^{\rm ef}$	$0.9\pm0.1^{\rm f}$	$120.3\pm3.6^{\rm efg}$	$110.4\pm6.1^{\rm de}$
	70	8.3 ± 0.5^g	$400.0\pm0.0^{\rm g}$	47.4 ± 2.6^{8}	$116.9\pm5.8^{\rm h}$	$0.9 \pm 0.0^{\mathrm{cdef}}$	$92.5\pm4.9^{\rm i}$	83.2 ± 5.2^{f}
Blend 5	09	$10.5\pm0.5^{\rm c}$	$633.3 \pm 61.7^{\mathrm{d,e}}$	$80.3 \pm 3.9^{\rm b}$	$149.1\pm7.8^{\rm f}$	$1.0\pm0.0^{\rm abc}$	$112.5\pm6.9^{\rm gh}$	$108.0\pm8.8^{\rm de}$
(55SPI:40LF:5LPI)	65	$9.0\pm0.0^{\rm f}$	406.7 ± 45.8^{g}	$60.4 \pm 2.3^{\rm e}$	$146.6\pm5.2^{\rm f}$	$0.9\pm0.0^{\mathrm{def}}$	$120.0\pm4.3^{\rm egf}$	$109.2\pm6.1^{\rm de}$
	70	$8.0 \pm 0.0^{\text{g}}$	$292.9 \pm 26.7^{\rm h}$	$46.0\pm2.1~\mathrm{g.h}$	89.5 ± 8.2^{j}	$0.9\pm0.0^{\mathrm{cdef}}$	$71.7 \pm 6.8^{\rm j}$	$65.9 \pm 5.9^{\rm h}$
Blend 6	09	$11.0\pm0.0^{\rm f}$	$900.0\pm0.0^{\rm b}$	$81.0\pm0.0^{\rm b}$	176.3 ± 6.2^{cd}	$0.9\pm0.1^{\text{b-f}}$	$134.7 \pm 6.0^{\circ}$	$124.5 \pm 8.3^{\circ}$
(55SPI:35LF:10LPI)	65	$9.5\pm0.5^{\rm e}$	673.3 ± 70.4^{d}	$60.8 \pm 3.3^{\circ}$	$149.4\pm38^{\mathrm{f}}$	$0.9\pm0.0^{\mathrm{f}}$	$121.7\pm3.0^{\rm ef}$	$109.7 \pm 4.7^{\mathrm{de}}$
	70	8.0 ± 0.0^{g}	420.0 ± 41.4^{g}	$43.9\pm0.0^{\rm h}$	$105.6\pm4.7^{\mathrm{i}}$	$0.9\pm0.0^{\text{b-f}}$	$85.1\pm3.6^{\rm i}$	77.7 ± 5.7^{fg}
		30.4.30	1					

Abbreviations: FMC, feed moisture content; SME, specific mechanical energy; SPI, soy protein isolate; LF, lupin flour; LPI, lupin protein isolate. Note: Data is expressed as mean \pm standard deviation (n = 9). Different letters in a column are significantly different (p < 0.05).

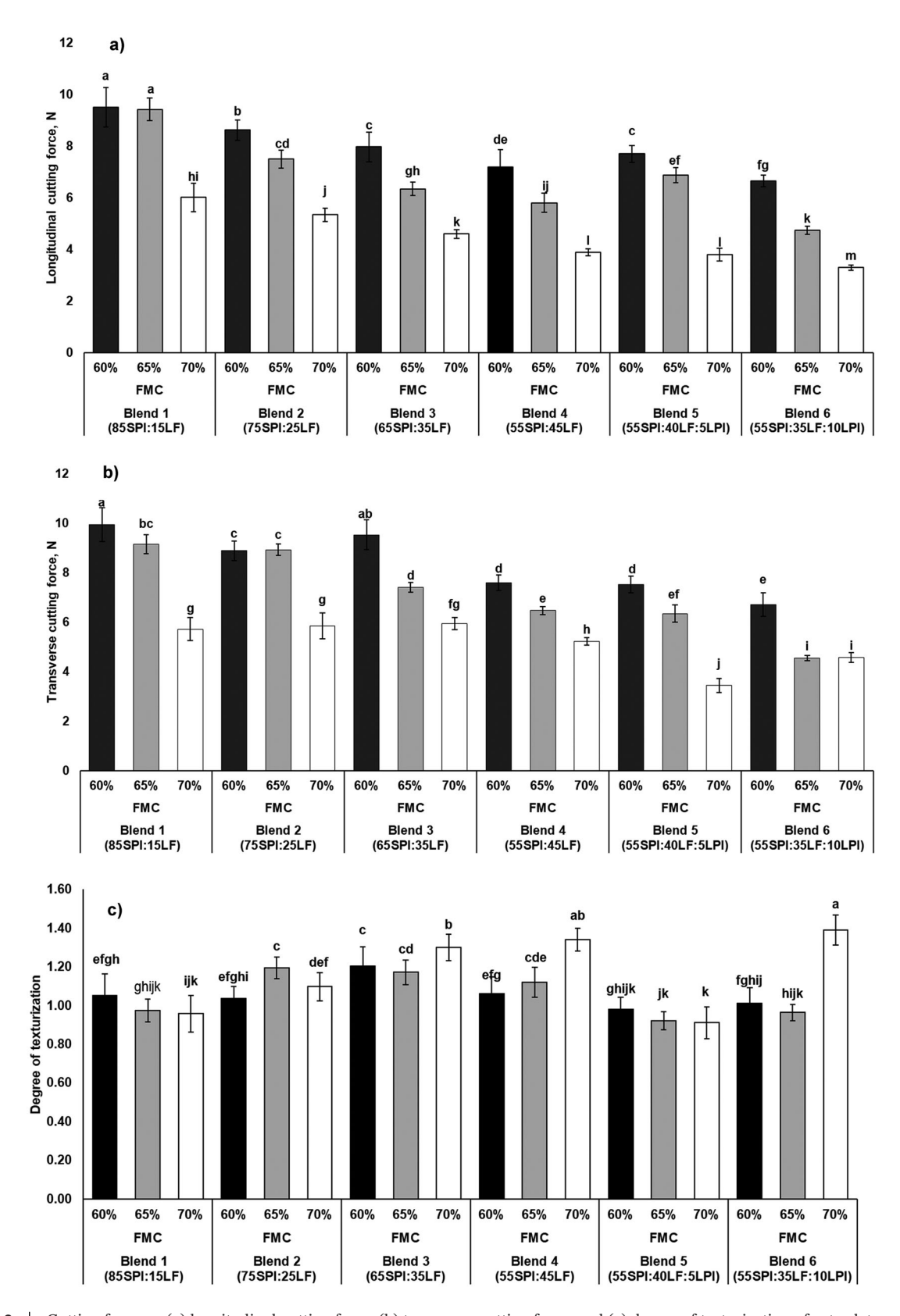


FIGURE 2 Cutting force on (a) longitudinal cutting force, (b) transverse cutting force, and (c) degree of texturization of extrudates produced by different formulas, and different moisture contents treatments. Errors bars represent \pm standard deviation (n = 9). Different letters on bars in each sub-figure reflect significant differences (p < 0.05).

The degree of texturization (DT) values greater than 1 typically indicate the formation of fiber-like structures within the cooling die in the extrudate flow direction (Chiang et al. 2020). In this study, all HMMAs exhibited fibrous structures across all the FMC levels, with approximately two-thirds of the HMMAs showing DT values greater than 1 (Figure 2c). The highest degree of texturization was observed for HMMAs produced from blends 3, 4, and 6 at 70% FMC, with DT values of 1.3, 1.3, and 1.4, respectively. These values are comparable to those reported by Mohamad Mazlan et al. (2020) for chicken meat, where breast and drumstick had DT values of 1.26 and 1.23, respectively.

Higher DT observed in HMMAs made from blends with higher LF concentrations can be attributed to the decreasing protein content and increasing carbohydrate content. Kaleda et al. (2021) found that lowering the protein content from 78.6% to 63.5% while increasing carbohydrates from 4.9% to 17.3% led to the development of more fibrous structures in meat analogues made from oat-pea protein blends. Similarly, Pietsch et al. (2019) demonstrated that during high-moisture extrusion of soy protein concentrate, components like polysaccharides and their structural changes played a key role in altering the melt's rheological properties, which contributed to the formation of anisotropic structures in the HMMAs. While a higher protein concentration in the raw materials allows for more cross-linking, creating a denser protein network, it doesn't necessarily result in improved fiber formation (Kantanen et al. 2022). This likely explains why HMMAs produced from blends with lower protein content (blends 3, 4, and 6) exhibited improved texturization compared to those with higher protein content (blends 1 and 2). The enhanced fibrous structure observed in blends with higher lupin protein content suggests potential for applications where proteinpolysaccharide interactions are key to matrix formation, as also demonstrated in edible film systems incorporating modified myofibrillar proteins and cellulose nanocrystals (Chen et al. 2023).

The TPA parameters of the HMMAs are summarized in Table 4. Regardless of the blend formulation, TPA attributes such as hardness, gumminess, and chewiness demonstrated a decreasing trend with increasing FMC. This reduction can be attributed to a lower protein matrix density at higher FMC, resulting in softer textures, aligning with previous reports on HMMAs produced from hemp (Rajendra et al. 2023) and soy-sunflower meal (Singh et al. 2024). Similarly, da Silva et al. (2024) observed a decrease in hardness and chewiness of brewers' spent grain incorporated soy HMMAs at higher FMC. They also reported an increase in TPA attributes with increasing protein content and decreasing carbohydrate content, which is consistent with the findings of this study. This may be due to the greater influence of proteincarbohydrate interactions over protein-protein interactions in shaping the rheology of the melt and the textural properties of the end product when the raw material contains a substantial amount of carbohydrates (da Silva et al. 2024; Pietsch et al. 2019). One exception to this trend was the HMMAs from blend 2. The deviation observed in Blend 2 HMMAs may be due to an optimal SPI-to-LF ratio at which water absorption and viscosity of the melt were likely enhanced, as evident from the final viscosity of Blend 2 (Table 3). This increased viscosity may have resulted in higher SME input during extrusion and increased hardness of the end product (Zahari et al. 2023). However, as LF content was further in Blends 3–6, the excess carbohydrates and fibers may have disrupted the protein network, weakening the matrix and leading to lower SME input during extrusion and a softer end product (Schmid et al. 2022).

When comparing blend formulations, blends 1 and 2 consistently exhibited higher hardness, gumminess, and chewiness values across all FMC levels compared to blends 3–6, with blend 2 showing the highest values in all cases. A similar trend was observed for the SME values, where blend 2 consistently demonstrated the highest SME values. A positive correlation between SME and HMMA textural attributes has also been reported by Chen et al. (2010), Palanisamy et al. (2019), and Singh et al. (2024).

Overall, both FMC and blend formulation significantly impacted the textural properties, with higher FMC and LF content contributing to softer textures. This could be due to the enhanced protein-carbohydrate interactions resulting from the high carbohydrate content in LF. Additionally, extrusion cooking was found to break down the glycosidic bonds of insoluble dietary fibers and convert them into smaller, soluble fractions (Huang and Ma 2016; Jing and Chi 2013). An increase in soluble fiber fraction, as discussed previously, can enhance the water-binding capacity of HMMAs, resulting in a softer, mushier texture (Naumann et al. 2021; Schreuders et al. 2022). The decrease in hardness with increasing LF concentration could also be attributed to the larger particle size of LF, which may have disrupted the protein matrix, leading to weaker protein-protein interactions (Pang et al. 2021). The differences in textural properties with varying LF concentrations could also be attributed to its higher oil content compared to SPI. An increased oil content may interfere with protein polymerization processes during extrusion, leading to a weaker protein network structure (Kendler et al. 2021). The softer and less chewy texture of HMMAs produced at elevated FMC and LF levels may make them more suitable for elderly people, who often experience difficulty consuming firmer and chewier foods.

3.6 | Color Analysis

The color attributes of the raw blends and the HMMAs are presented in Table 5. A reduction in L* values, alongside increases in both a* and b* values, was observed in all HMMAs compared to their raw blends, indicating darker color after extrusion. This darkening with extrusion cooking can be attributed to the Maillard reaction products formed during high-temperature processing (Ilo and Berghofer 1999).

The HMMAs from blend 1 were lighter (higher L*) compared to other blends, particularly at higher FMCs, which can be attributed to the lighter color of its raw material blend. However, this difference was only significant (p < 0.05) at 70% FMC. In terms of a* and b* values, HMMAs exhibited generally richer red (higher a*) and yellow (higher b*) colors compared to the raw material blends. However, no consistent trends were observed for a* and b* values of HMMAs as a function of FMC and blend composition. While for most of the HMMAs, the FMC did not have a significant (p < 0.05) effect, significant differences (p < 0.05) in color attributes of HMMAs were noted for blend 3 between 60% and 65% FMC, for blend 5 between 60% and 70% FMC, and for blend 6 between 65% and 70% FMC.

TABLE 5 Color parameters (L*, a*, b*, ΔE) of the raw material blends and the HMMAs produced at different feed moisture contents (FMCs).

			•		
	FMC %	L*	a*	b*	ΔΕ
	Raw material	84.4 ± 0.2^{a}	$0.8 \pm 0.0^{\rm g}$	16.0 ± 0.1^{k}	_
Blend 1 (85SPI:15LF)	60	$53.0 \pm 0.1^{\circ}$	$3.6 \pm 0.3^{a-e}$	23.0 ± 1.0^{bcde}	$32.3 \pm 0.7^{a-e}$
	65	50.3 ± 1.0^{cd}	$3.1 \pm 0.4^{\mathrm{def}}$	$21.5 \pm 0.2^{\rm defg}$	$32.2 \pm 0.9^{a-e}$
	70	$53.3 \pm 0.8^{\circ}$	$2.8 \pm 0.3^{\rm f}$	$20.5 \pm 0.5^{\rm fgh}$	31.5 ± 0.2^{e}
Blend 2	Raw material	83.9 ± 0.2^{ab}	0.9 ± 0.0^{g}	17.0 ± 0.2^{jk}	_
	60	$50.3 \pm 1.6^{\rm efgh}$	3.3 ± 0.3 b-f	$21.6 \pm 1.2^{\rm def}$	34.0 ± 0.5^{abcd}
(75SPI:25LF)	65	$52.5 \pm 0.8^{\text{cde}}$	$2.9 \pm 0.1^{\rm ef}$	$21.5 \pm 0.3^{\rm defg}$	$31.8 \pm 0.8^{\rm de}$
	70	$52.1 \pm 0.4^{\rm cdef}$	$2.8 \pm 0.3^{\rm f}$	$20.9 \pm 1.3^{\rm efg}$	$32.1 \pm 1.7^{\text{bcde}}$
Blend 3 (65SPI:35LF)	Raw material	83.5 ± 0.2^{ab}	$1.0 \pm 0.1^{\rm g}$	17.7 ± 0.5^{ijk}	_
	60	$49.6\pm0.4^{\rm ghi}$	3.7 ± 0.3^{abcd}	22.9 ± 0.5^{bcde}	34.4 ± 1.2^{abc}
	65	52.7 ± 0.8^{cd}	$3.2 \pm 0.4^{\mathrm{def}}$	$22.3 \pm 0.5^{\rm cdef}$	31.2 ± 0.2^{e}
	70	$52.0 \pm 1.33^{\text{cdef}}$	$3.1 \pm 0.3^{\mathrm{def}}$	$23.9 \pm 0.9^{\rm abcd}$	$32.1 \pm 0.3^{\text{bcde}}$
	Raw material	83.4 ± 0.1^{ab}	$1.0 \pm 0.1^{\rm g}$	$18.3 \pm 0.3^{\rm hij}$	-
Blend 4 (55SPI:45LF)	60	$49.9 \pm 0.7^{\rm fghi}$	4.0 ± 0.3^{abc}	$23.4 \pm 0.4^{\rm abcd}$	34.0 ± 0.2^{abc}
	65	$52.4 \pm 0.5^{\text{cde}}$	$3.2 \pm 0.4^{a-f}$	24.2 ± 1.2^{abc}	$31.6 \pm 0.4^{\mathrm{de}}$
	70	$51.9 \pm 0.3^{c-g}$	$4.0 \pm 0.2^{\text{cdef}}$	23.7 ± 0.5^{abcd}	$32.0 \pm 0.6^{\text{cde}}$
Blend 5	Raw material	82.7 ± 0.1^{ab}	1.063 ± 0.1^{g}	$18.3 \pm 0.3^{\rm hijk}$	-
	60	48.7 ± 1.6^{hi}	4.0 ± 0.3^{ab}	24.4 ± 0.8^{abc}	34.7 ± 0.6^{a}
(55SPI:40LF:5LPI)	65	$50.2 \pm 0.4^{\rm efgh}$	3.8 ± 0.1^{abc}	25.0 ± 0.6^{ab}	$33.3 \pm 0.2^{a-e}$
	70	$51.5 \pm 0.6^{\text{c-g}}$	$3.5 \pm 0.2^{a-f}$	25.4 ± 0.8^{a}	$32.1 \pm 1.6^{\rm bcde}$
	Raw material	82.0 ± 0.4^{b}	$1.288\pm0.1^{\rm g}$	$19.3 \pm 0.2^{\rm ghi}$	-
Blend 6	60	47.9 ± 0.6^{i}	4.1 ± 0.1^{a}	$24.2 \pm 1.6^{\rm abc}$	34.5 ± 0.4^{ab}
(55SPI:35LF:10LPI)	65	$51.1 \pm 0.7^{\text{c-g}}$	3.8 ± 0.0^{abcd}	24.4 ± 0.4^{abc}	31.5 ± 0.6^{e}
	70	$50.5 \pm 0.4^{d-h}$	$3.5 \pm 0.2^{a-f}$	24.0 ± 1.6^{abc}	$31.9 \pm 0.8^{\rm cde}$

Note: Data is presented as mean \pm standard deviation (n = 3). In each column, values assigned with different letters are significantly different (p < 0.05). Abbreviations: FMC, feed moisture content; SPI, soy protein isolate; LF, lupin flour; LPI, lupin protein isolate.

The HMMAs made from blends incorporating LPI (blends 5 and 6) exhibited slightly darker color compared to those without LPI. During alkaline extraction of LPI, phenolic compounds can oxidize into quinones, which then interact with free $\rm NH_2$ or thiol groups, forming dark pigments through condensation. Therefore, this variation in color may be linked to the reaction between quinones and amino acid residues (Ramos-Diaz et al. 2023).

Significant (p < 0.05) color differences (ΔE) were observed between all raw material blends and their corresponding HMMAs. For all the blends studied, an increase in FMC resulted in significantly (p < 0.05) lower ΔE values, indicating that higher FMC reduced the overall color difference between the raw materials and the HMMAs. This can be explained by the lubricating effect of water, which reduces mechanical energy input (Table 4) and, consequently, the extent of Maillard reactions during extrusion processing (Chen et al. 2010; Palanisamy et al. 2019; Saldanha do Carmo et al. 2021). In addition, water may alter the color intensity by diluting the water-soluble color components (Wi et al. 2020). Palanisamy et al. (2019) also observed that higher FMC led to lighter products and reduced color differences (ΔE) between raw materials and HMMAs, aligning with our

findings. These findings suggest that optimizing FMC and blend composition is crucial for achieving desired color attributes in plant-based meat alternatives.

3.7 | Macrostructure of the HMMAs

The macrostructure of the HMMAs produced from different raw material blends at varying FMCs is presented in Figure 3. The visual inspection of the HMMAs indicated that the blend composition and FMC significantly influenced the structural properties of the extrudates. Blends with higher SPI content (blends 1 and 2) demonstrated better fibrous structure (higher DT) at lower FMCs, consistent with effective texturization due to higher protein content facilitating network formation. This aligns with previous findings where higher protein content in soy protein blends enhanced fiber formation in HMMAs (Lin et al. 2000). Blend 3-6 showed a fibrous but scaly appearance at 60% FMC, with the fibrous structure becoming more pronounced at 65% and 70% FMC, indicating that higher LF content can support fiber formation at higher FMC levels. This finding aligns with the observations by Saldanha do Carmo et al. (2021).



FIGURE 3 | Visual appearance of SPI-LF and SPI-LF-LPI high-moisture meat analogues. SPI: soy protein isolate, LF: lupin flour, LPI: lupin protein isolate.

Visual differences in the macrostructure of HMMAs appeared closely linked to their textural properties and moisture content. Samples exhibiting more pronounced and continuous fibrous structures, particularly those extruded at higher FMCs and with higher lupin content (e.g., blends 3, 4, and 6), were easier to cut, i.e., lower peak cutting force, and better texturized, i.e., higher degree of texturization (DT). In contrast, HMMAs with less organized structures or scaly appearances (noted in blends with high SPI content at lower FMCs) exhibited

higher hardness, gumminess, and peak cutting force values, indicative of a denser, drier matrix. These observations suggest that macrostructural organization of HMMAs has implications on the water-HMMA matrix interactions and the mechanical resistance of the HMMAs to deformation. Therefore, tailoring fiber formation during high-moisture extrusion cooking is critical not only for replicating meat-like textures but also for optimizing moisture retention and enhancing sensory appeal.

TABLE 6 | Degree of proteolysis (%) of the raw material blends and the HMMAs produced at different feed moisture contents (FMCs).

	FMC (%)	Degree of proteolysis (%)
Blend 1	Raw material	$33.3 \pm 2.0^{\rm e}$
(85SPI:15LF)	60	$33.3 \pm 2.1^{\rm e}$
	70	36.2 ± 1.2^{d}
Blend 2	Raw material	$38.0 \pm 1.8^{\rm cd}$
(75SPI:25LF)	60	36.7 ± 2.2^{cd}
	70	$39.2 \pm 1.6^{\circ}$
Blend 3	Raw material	$39.6 \pm 1.7^{\circ}$
(65SPI:35LF)	60	36.7 ± 1.2^{cd}
	70	44.4 ± 3.9^{b}
Blend 4 (55SPI:45LF)	Raw material	42.3 ± 2.0^{bc}
	60	42.5 ± 2.8^{bc}
	70	51.5 ± 2.8^{a}

Note: The number following the \pm sign refers to standard deviation (n = 3). Values assigned with different letters are significantly different (p < 0.05). Abbreviation: FMC, feed moisture content; SPI, soy protein isolate; LF, lupin flour.

3.8 | In vitro Protein Digestibility

The results of In vitro protein digestion of the raw blends revealed significant (p < 0.05) differences as a function of SPI to LF ratio. As the proportion of LF increased and SPI decreased going from blend 1 to 4, the degree of proteolysis increased. Blend 4 exhibited the highest protein digestibility (51.5%), likely due to the excellent digestibility of lupin proteins (Aguilera et al. 1985). This may be associated with the low levels of anti-nutritional factors in lupin (Monteiro et al. 2014).

Extrusion generally improves protein digestibility by inactivating anti-nutritional factors and thermal denaturation of proteins. Denaturation unfolds the protein, allowing more extensive hydrolysis by digestive enzymes (Gulati et al. 2020). For instance, Öztürk et al. (2024) reported that high moisture extrusion improved the In vitro protein digestibility of sunflower protein by approximately 30%. This aligns with the current results, where protein digestibility increased after extrusion.

The degree of proteolysis of the HMMAs was also dependent on FMC (Table 6). HMMAs produced at 70% FMC had a significantly (p < 0.05) higher degree of proteolysis compared to those at 60% FMC. This trend aligns with the findings of Palanisamy et al. (2019), who reported that increasing FMC (from 40% to 68%) significantly enhanced In vitro protein digestibility. Chen et al. (2011) proposed that higher FMC during extrusion reduces the protein polymerization and enhances the accessibility of proteins to digestive enzymes. Shan et al. (2023) observed that increased FMC results in softer HMMAs that swell faster in the gastrointestinal environment, allowing more contact area with digestive proteases. Similarly, in this study, as HMMAs became softer (i.e., lower hardness), the degree of proteolysis increased.

3.9 | Antioxidant Capacity

While many studies emphasize developing meat analogues with high textural quality, fewer address their potential as functional foods. Antioxidant capacity is a key measure of functionality, as it plays a crucial role in reducing oxidative stress, which is linked to the onset of various chronic diseases. Beyond its health benefits, antioxidant capacity is also critical for assessing oxidative stability and inhibiting rancidity, both of which are essential for extending product shelf life (Sha and Xiong 2020). By preventing lipid oxidation, antioxidants contribute to maintaining the quality and sensory attributes of meat analogues, making them more viable for commercial applications. Figures 4a and b illustrate the antioxidant capacities of the raw blends, measured using ABTS and ORAC-FL assays, while Figures 4c and d show the antioxidant capacities of the HMMAs using the same methodologies. Extrusion significantly reduced (p < 0.05) the antioxidant capacity in all HMMAs (Figures 4 a, b, c, and d). For the results obtained using the ABTS method, the antioxidant capacity decreased from an average of 50 µmol TE/g in the raw blends to values below 25 µmol TE/g in the extruded samples. For the results obtained using the ORAC method, the reduction was from values above 150 µmol TE/g in the raw sample to values below 100 µmol TE/g in the extruded samples. This can be attributed to the high temperature, pressure, and shear forces within the extruder barrel, which degrade thermolabile antioxidant compounds (Ling et al. 2022). These findings align with studies reporting reduced total phenolic content and antioxidant capacity after extrusion (Estivi et al. 2023; Ruiz-Gutiérrez et al. 2015). Although antioxidant capacity was decreased following the extrusion cooking process, a substantial level of antioxidant activity was retained across all HMMA samples. This residual antioxidant activity may contribute not only to technological benefits, such as extended product shelf life through oxidative stability, but also to potential nutritional advantages associated with antioxidant intake.

The analysis of the raw materials revealed that Blend 1 exhibited the highest antioxidant capacity (p < 0.05) in the ABTS assay, which significantly decreased (p < 0.05) after digestion. A similar trend was observed for Blends 2 and 4, whereas Blend 3 showed no significant differences after digestion. In contrast, the ORAC-FL assay revealed an increase in antioxidant capacity across all raw material blends post-digestion. The ORAC-FL and ABTS assays demonstrated differing antioxidant activity profiles between blends. This could be attributed to the specific sensitivity of ORAC-FL to hydrophilic antioxidants (Huang et al. 2002). These methodological differences highlight the importance of employing multiple assays to obtain a comprehensive antioxidant profile. Among the different methods employed, ORAC-FL is considered more biologically relevant and serves as a benchmark for antioxidant capacity (Munteanu and Apetrei 2021).

Interestingly, i vitro digestion enhanced the antioxidant capacity of all the HMMAs (Figure 4c, 4d). This improvement is likely due to the release of peptides and other bioactive compounds capable of neutralizing free radicals during digestion (Correa et al. 2022; Fillería et al. 2021). Simulated digestive conditions enable the release of these compounds, enhancing their activity. FMC also

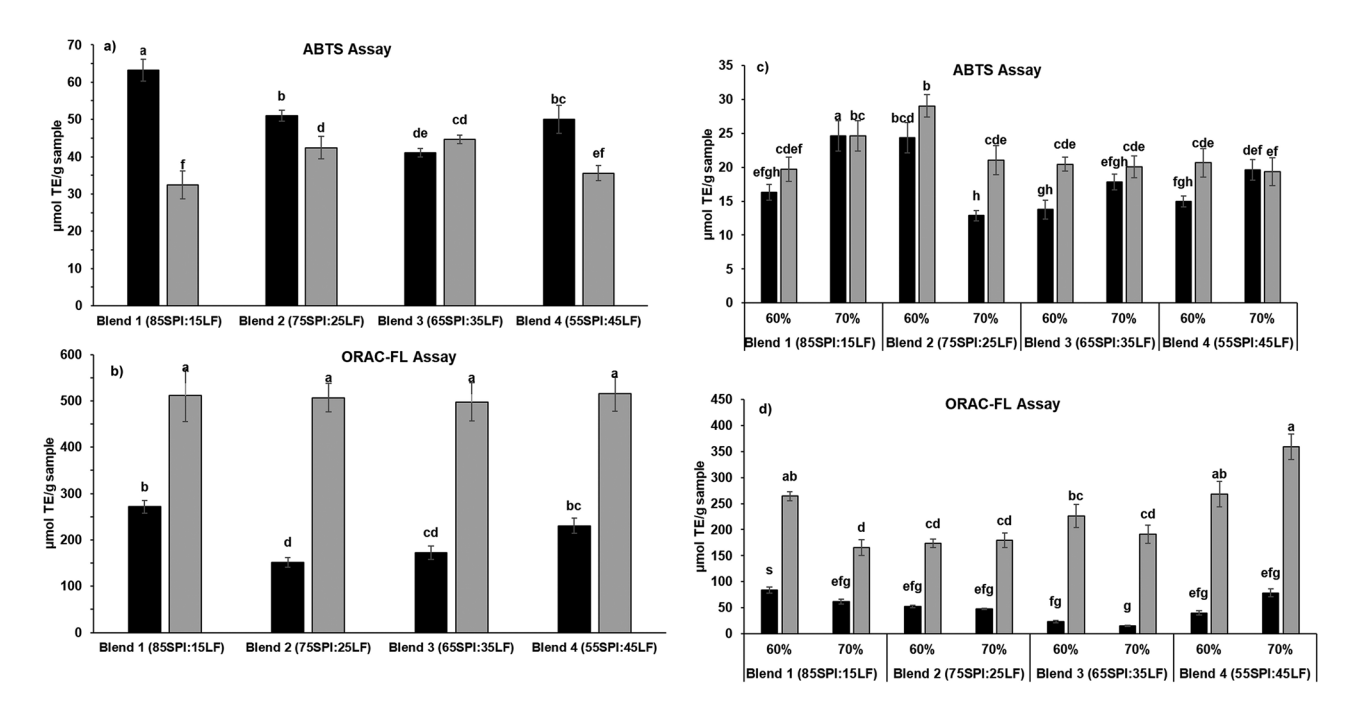


FIGURE 4 Antioxidant capacity of raw blends (a and b) and HMMAs (c and d) before () and after () digestion assessed by ABTS $^{\bullet}$ + and ORAC-FL assay. Error bars represent \pm standard deviation (n = 3). Values assigned with different letters are significantly different (p < 0.05).

played a critical role in the antioxidant capacity of the HMMAs. This effect was most evident in the results obtained using the ORAC-FL assay, where blends extruded at 70% FMC exhibited higher antioxidant activity, particularly in digested samples, compared to those extruded at 60% FMC. This protective effect of higher FMC on antioxidant compounds could be attributed to the lower viscosity within the extruder barrel at elevated moisture levels (Brennan et al. 2011; Ortiz et al. 2018).

Overall, the results highlight the importance of considering not only the initial antioxidant content of foods but also the impact of processing and digestion on antioxidant retention and bioavailability. In vitro digestion findings demonstrate that, despite reductions during extrusion, lupin-based HMMAs can still deliver bioaccessible antioxidant compounds. These results suggest that extrusion-processed plant-based meat analogues may retain functional properties post-consumption, contributing to both product stability and potential health benefits through oxidative stress mitigation. Future studies should explore the bioavailability and in vivo effects of these bioaccessible antioxidants to fully elucidate their role in promoting human health.

4 | Conclusion

This study successfully demonstrated the potential of LF and LPI in the development of HMMAs through extrusion cooking. Higher FMC reduced extrusion torque and die pressure and thereby the SME. Texture analysis indicated that increasing LF content reduced hardness and produced softer, more tender HMMAs, which are likely more suitable for elderly people. The DT values ranging from 1.0 to 1.4 confirmed the formation of fibrous structures, particularly at higher FMC. Extrusion at 70% FMC significantly improved In vitro protein digestibility, with

the highest degree of proteolysis (51.5%) observed in blend 4, containing the highest amount of LF. Antioxidant compounds in the HMMAs persisted after digestion, potentially contributing to the mitigation of oxidative stress, a key factor in chronic diseases. The bioaccessibility of these compounds suggests their potential to counteract oxidative damage. ORAC-FL analysis revealed an increase in antioxidant capacity of the HMMAs post-digestion, highlighting the importance of using multiple assays for the measurement of antioxidant capacity of foods. These findings highlight the potential of *Lupinus angustifolius* as a sustainable, nutrient-dense ingredient for developing functional foods with antioxidant properties and plant-based meat alternatives.

From an economic perspective, the use of LF over LPI presents a more cost-effective and practical alternative due to lower processing requirements and higher mass yield. LF reduces production costs while also adding dietary fiber and other nutrients, thereby enhancing product nutritional and functional quality. From an environmental perspective, lupin enhances sustainability through nitrogen fixation. Its local sourcing offers a lower-carbon alternative to imported soy. The integration of LF with SPI enables the development of HMMAs with desirable texture and nutrition while supporting the transition towards more sustainable, affordable plant-based protein sources. HMMAs from blends containing LF exhibited superior or comparable textural attributes compared to the ones containing LPI, highlighting the suitability of the SPI-LF combination for the creation of relatively more sustainable products with high fiber levels and desirable textural properties. By leveraging SPI as a key structuring component, this study demonstrates its potential to support the formation of fibrous networks while accommodating a high proportion of native LF. These insights pave the way for the development of innovative and more sustainable food products that align with global health and environmental goals.

Future research will focus on the identification and quantification of phenolic compounds, amino acids, tocopherols, and carotenoids in lupin-based HMMAs, as well as their bioavailability through cellular studies. In vitro analyses will evaluate their antioxidant potential, while cellular assays will be conducted on the bioaccessible fraction to further investigate its functional properties. Additionally, the impact of the non-bioaccessible insoluble fraction on gut microbiota will be assessed. Furthermore, the evaluation of antinutritional factors will provide a more comprehensive perspective on the nutritional quality of these HMMAs. Additionally, sensory evaluation (e.g., using Check-All-That-Apply (CATA) and Just-About-Right (JAR) methodologies) can be conducted to further optimize key texture and flavor attributes and enhance overall consumer acceptability, ensuring the market viability of these lupin-based HMMAs. Studies focusing on microstructural characteristics and protein quality will provide critical insights for nutritional claims and industrial applications, as the microstructure of HMMAs is closely linked to textural attributes. Understanding these relationships can help optimize processing conditions to achieve desirable textures while maintaining protein quality. Additionally, investigating different processing techniques, such as 3D printing and incorporating other plant proteins, could further enhance the functionality and appeal of lupin-based meat alternatives.

Author Contributions

Matias Rodriguez Elhordoy: writing – original draft, writing – review and editing, formal analysis, methodology, investigation, visualization. Aayushi Kadam: investigation, writing – original draft, writing – review and editing, methodology, formal analysis, supervision, visualization. Daniel Vazquez: writing – review and editing, conceptualization, supervision, visualization. Alejandra Medrano: writing – review and editing, conceptualization, funding acquisition, supervision, visualization, validation, investigation, project administration. Filiz Koksel: conceptualization, investigation, funding acquisition, writing – review and editing, visualization, validation, supervision, project administration.

Acknowledgments

The financial support for this project was provided by the Natural Sciences and Engineering Research Council (NSERC) Canada, Discovery Grants program for F. Koksel. Infrastructural support was provided by the Canada Foundation for Innovation (CFI) JELF program. Additional financial support was received from the Agencia Nacional de Investigación e Innovación (ANII) MR through scholarships POS_NAC_2022_1_174183 and MOV_CA_2021_171688; Programa de Desarrollo de las Ciencias Básicas (PEDECIBA); and Comisión Sectorial de Investigación Científica through Project 22420230100104UD.

Conflicts of Interest

The authors declare no conflicts of interest.

Data Availability Statement

No datasets were generated or analyzed during the current study.

References

AACC International. 2010. AACC Approved Methods of Analysis, 11th ed. American Association Of Cereal Chemists.

Aguilera, J. F., E. Molina, and C. Prieto. 1985. "Digestibility and Energy Value of Sweet Lupin Seed (*Lupinus albus* var. Multolupa) in Pigs."

Animal Feed Science and Technology 12, no. 3: 171–178. https://doi.org/10. 1016/0377-8401(85)90010-0.

Albe-Slabi, S., O. Mesieres, C. Mathé, M. Ndiaye, O. Galet, and R. Kapel. 2022. "Combined Effect of Extraction and Purification Conditions on Yield, Composition and Functional and Structural Properties of Lupin Proteins." *Foods* 11, no. 11: 1646. https://doi.org/10.3390/foods11111646.

AOAC. 2005. Official method of Analysis, 18th ed. Association of Officiating Analytical Chemists, Washington, DC.

Badjona, A., B. Cherono, R. Bradshaw, and B. Dubey. 2025. "Gelation and Rheological Properties of Ultrasound-Extracted Faba Bean Protein: A Comparative Study With Commercial Plant Proteins." *Food Hydrocolloids* 162: 110997. https://doi.org/10.1016/j.foodhyd.2024.110997.

Báez, J., A. M. Fernández-Fernández, V. Tironi, M. Bollati-Fogolín, M. C. Añón, and A. Medrano-Fernández. 2021. "Identification and Characterization of Antioxidant Peptides Obtained From the Bioaccessible Fraction of α -lactalbumin Hydrolysate." *Journal of Food Science* 86, no. 10: 4479–4490. https://doi.org/10.1111/1750-3841.15918.

Bähr, M., A. Fechner, K. Hasenkopf, S. Mittermaier, and G. Jahreis. 2014. "Chemical Composition of Dehulled Seeds of Selected Lupin Cultivars in Comparison to Pea and Soya Bean." *LWT—Food Science and Technology* 59, no. 1: 587–590. https://doi.org/10.1016/j.lwt.2014.05.026.

Barton, L., T. Thamo, D. Engelbrecht, and W. K. Biswas. 2014. "Does Growing Grain Legumes or Applying Lime Cost Effectively Lower Greenhouse Gas Emissions From Wheat Production in a Semi-Arid Climate?" *Journal of Cleaner Production* 83: 194–203. https://doi.org/10.1016/j.jclepro.2014.07.020.

Berghout, J. A. M., R. M. Boom, and A. J. van der Goot. 2014. "The Potential of Aqueous Fractionation of Lupin Seeds for High-Protein Foods." *Food Chemistry* 159: 64–70. https://doi.org/10.1016/j.foodchem. 2014.02.166.

Beyer, H., A. K. Schmalenberg, G. Jansen, et al. 2015. "Evaluation of Variability, Heritability and Environmental Stability of Seed Quality and Yield Parameters of *L. angustifolius*." *Field Crops Research* 174: 40–47. https://doi.org/10.1016/j.fcr.2014.12.009.

Brennan, C., M. Brennan, E. Derbyshire, and B. K. Tiwari. 2011. "Effects of Extrusion on the Polyphenols, Vitamins and Antioxidant Activity of Foods." *Trends in Food Science & Technology* 22, no. 10: 570–575. https://doi.org/10.1016/j.tifs.2011.05.007.

Bressiani, J., G. S. Santetti, T. Oro, et al. 2021. "Hydration Properties and Arabinoxylans Content of Whole Wheat Flour Intended for Cookie Production as Affected by Particle Size and Brazilian Cultivars." *LWT* 150: 111918. https://doi.org/10.1016/j.lwt.2021.111918.

Brodkorb, A., L. Egger, M. Alminger, et al. 2019. "INFOGEST Static in Vitro Simulation of Gastrointestinal Food Digestion." *Nature Protocols* 14, no. 4: 991–1014. https://doi.org/10.1038/s41596-018-0119-1.

Cháirez-Jiménez, C., C. Castro-López, S. Serna-Saldívar, and C. Chuck-Hernández 2023. "Partial Characterization of Canola (Brassica napus L.) Protein Isolates as Affected by Extraction and Purification Methods." *Heliyon* 9, no. 11: e21938. https://doi.org/10.1016/j.heliyon.2023.e21938.

Chen, F. L., Y. M. Wei, and B. Zhang. 2011. "Chemical Cross-Linking and Molecular Aggregation of Soybean Protein During Extrusion Cooking at Low and High Moisture Content." *LWT* 44, no. 4: 957–962. https://doi.org/10.1016/j.lwt.2010.12.008.

Chen, F. L., Y. M. Wei, B. Zhang, and A. O. Ojokoh. 2010. "System Parameters and Product Properties Response of Soybean Protein Extruded at Wide Moisture Range." *Journal of Food Engineering* 96, no. 2: 208–213. https://doi.org/10.1016/j.jfoodeng.2009.07.014.

Chen, J., J. Chai, X. Chen, M. Huang, X. Zeng, and X. Xu. 2023. "Development of Edible Films by Incorporating Nanocrystalline Cellulose and Anthocyanins Into Modified Myofibrillar Proteins." *Food Chemistry* 417: 135820. https://doi.org/10.1016/j.foodchem.2023.135820.

Chiang, J. H., A. K. Hardacre, and M. E. Parker. 2020. "Extruded Meat Alternatives Made from Maillard-Reacted Beef Bone Hydrolysate and

Plant Proteins: Part I – Effect of Moisture Content." *International Journal of Food Science & Technology* 55, no. 2: 649–659. https://doi.org/10.1111/ijfs. 14319.

Correa, J. L., J. E. Zapata, and B. Hernández-Ledesma. 2022. "Release of Bioactive Peptides From Erythrina Edulis (Chachafruto) Proteins Under Simulated Gastrointestinal Digestion." *Nutrients* 14, no. 24: 5256. https://doi.org/10.3390/nu14245256.

Cortés-Avendaño, P., M. Tarvainen, J.-P. Suomela, P. Glorio-Paulet, B. Yang, and R. Repo-Carrasco-Valencia. 2020. "Profile and Content of Residual Alkaloids in Ten Ecotypes of Lupinus Mutabilis Sweet After Aqueous Debittering Process." *Plant Foods for Human Nutrition* 75, no. 2: 184–191. https://doi.org/10.1007/s11130-020-00799-y.

daSilva, A. M. M., M. A. Lima, F. Koksel, and A. C. K. Sato. 2024. "Incorporation of Brewer's Spent Grain Into Plant-Based Meat Analogues: Benefits to Physical and Nutritional Quality." *International Journal of Food Science & Technology* 59, no. 6: 3870–3882. https://doi.org/10.1111/ijfs. 17134.

Dekkers, B. L., R. M. Boom, and A. J. van der Goot. 2018. "Structuring Processes for Meat Analogues." *Trends in Food Science and Technology* 81: 25–36. https://doi.org/10.1016/j.tifs.2018.08.011.

Dervas, G., G. Doxastakis, S. Hadjisavva-Zinoviadi, and N. Triantafillakos. 1999. "Lupin Flour Addition to Wheat Flour Doughs and Effect on Rheological Properties." *Food Chemistry* 66, no. 1: 67–73. https://doi.org/10.1016/S0308-8146(98)00234-9.

Devkota, L., K. Kyriakopoulou, R. Bergia, and S. Dhital. 2023. "Structural and Thermal Characterization of Protein Isolates From Australian Lupin Varieties as Affected by Processing Conditions." *Foods* 12, no. 5: 908. https://doi.org/10.3390/foods12050908.

Dikeman, C. L., and G. C. FaheyJr. 2006. "Viscosity as Related to Dietary Fiber: A Review." *Critical Reviews in Food Science and Nutrition* 46, no. 8: 649–663. https://doi.org/10.1080/10408390500511862.

Estivi, L., A. Brandolini, A. Gasparini, and A. Hidalgo. 2023. "Lupin as a Source of Bioactive Antioxidant Compounds for Food Products." *Molecules (Basel, Switzerland)* 28, no. 22: 7529. https://doi.org/10.3390/molecules28227529.

Ferchichi, N., W. Toukabri, U. Vrhovsek, et al. 2021. "Proximate Composition, Lipid and Phenolic Profiles, and Antioxidant Activity of Different Ecotypes of Lupinus albus, Lupinus Luteus and Lupinus Angustifolius." *Journal of Food Measurement and Characterization* 15, no. 2: 1241–1257. https://doi.org/10.1007/s11694-020-00722-8.

Fernández-Fernández, A. M., E. Dellacassa, T. Nardin, et al. 2021. "In Vitro Bioaccessibility of Bioactive Compounds From Citrus Pomaces and Orange Pomace Biscuits." *Molecules (Basel, Switzerland)* 26, no. 12: 3480. https://doi.org/10.3390/molecules26123480.

Fernández-Fernández, A. M., E. Dellacassa, T. Nardin, et al. 2022. "Tannat Grape Skin: A Feasible Ingredient for the Formulation of Snacks With Potential for Reducing the Risk of Diabetes." *Nutrients* 14, no. 3: 419. https://doi.org/10.3390/nu14030419.

Fernández-Fernández, A. M., E. Dumay, F. Lazennec, et al. 2021. "Antioxidant, Antidiabetic, and Antiobesity Properties, TC7-Cell Cytotoxicity and Uptake of Achyrocline Satureioides (Marcela) Conventional and High Pressure-Assisted Extracts." *Foods* 10, no. 4: 893. https://doi.org/10.3390/foods10040893.

Fillería, S. G., A. E. Nardo, M. Paulino, and V. Tironi. 2021. "Peptides Derived From the Gastrointestinal Digestion of Amaranth 11S Globulin: Structure and Antioxidant Functionality." Food Chemistry: Molecular Sciences 3: 100053. https://doi.org/10.1016/j.fochms.2021.100053.

Ghanghas, N., M. Nadimi, J. Paliwal, and F. Koksel. 2024. "Gas-Assisted High-Moisture Extrusion of Soy-Based Meat Analogues: Impacts of Nitrogen Pressure and Cooling Die Temperature on Density, Texture and Microstructure." *Innovative Food Science & Emerging Technologies* 92: 103557. https://doi.org/10.1016/j.ifset.2023.103557.

Guillermic, R.-M., A. J. Franczyk, S. O. Kerhervé, J. D. House, J. H. Page, and F. Koksel. 2023. "Characterization of the Mechanical Properties of

High-Moisture Meat Analogues Using Low-Intensity Ultrasound: Linking Mechanical Properties to Textural and Nutritional Quality Attributes." *Food Research International* 173: 113193. https://doi.org/10.1016/j.foodres. 2023.113193.

Gulati, P., S. Brahma, and D. J. Rose. 2020. "Chapter 13 - Impacts of Extrusion Processing on Nutritional Components in Cereals and Legumes: Carbohydrates, Proteins, Lipids, Vitamins, and Minerals." In *Extrusion Cooking*, edited by G. M. Ganjyal, 415–443. Woodhead Publishing. https://doi.org/10.1016/B978-0-12-815360-4.00013-4.

Hickisch, A., K. Bindl, R. F. Vogel, and S. Toelstede. 2016. "Thermal Treatment of Lupin-Based Milk Alternatives—Impact on Lupin Proteins and the Network of Respective Lupin-Based Yogurt Alternatives." *Food Research International* 89: 850–859. https://doi.org/10.1016/j.foodres.2016. 10.013.

Hickisch, A., R. Beer, R. F. Vogel, and S. Toelstede. 2016. "Influence of Lupin-Based Milk Alternative Heat Treatment and Exopolysaccharide-Producing Lactic Acid Bacteria on the Physical Characteristics of Lupin-Based Yogurt Alternatives." *Food Research International* 84: 180–188. https://doi.org/10.1016/j.foodres.2016.03.037.

Huang, D., B. Ou, M. Hampsch-Woodill, J. A. Flanagan, and E. K. Deemer. 2002. "Development and Validation of Oxygen Radical Absorbance Capacity Assay for Lipophilic Antioxidants Using Randomly Methylated Beta-Cyclodextrin as the Solubility Enhancer." *Journal of Agricultural and Food Chemistry* 50, no. 7: 1815–1821. https://doi.org/10.1021/jf01

Huang, Y.-L., and Y.-S. Ma. 2016. "The Effect of Extrusion Processing on the Physiochemical Properties of Extruded Orange Pomace." *Food Chemistry* 192: 363–369. https://doi.org/10.1016/j.foodchem.2015.07.039.

Hwang, N.-K., B.-J. Gu, Y. Zhang, and G.-H. Ryu. 2024. "Possibility of Isolated Mung Bean Protein as a Main Raw Material in the Production of an Extruded High-Moisture Meat Analog." *Foods* 13, no. 14: 2167. https://doi.org/10.3390/foods13142167.

Ilo, S., and E. Berghofer. 1999. "Kinetics of Colour Changes During Extrusion Cooking of Maize Grits." *Journal of Food Engineering* 39, no. 1: 73–80. https://doi.org/10.1016/S0260-8774(98)00148-4.

Jing, Y., and Y.-J. Chi. 2013. "Effects of Twin-Screw Extrusion on Soluble Dietary Fibre and Physicochemical Properties of Soybean Residue." *Food Chemistry* 138, no. 2: 884–889. https://doi.org/10.1016/j.foodchem.2012.12.003.

Kaleda, A., K. Talvistu, H. Vaikma, M.-L. Tammik, S. Rosenvald, and R. Vilu. 2021. "Physicochemical, Textural, and Sensorial Properties of Fibrous Meat Analogs From Oat-Pea Protein Blends Extruded at Different Moistures, Temperatures, and Screw Speeds." *Future Foods* 4: 100092. https://doi.org/10.1016/j.fufo.2021.100092.

Kantanen, K., A. Oksanen, M. Edelmann, et al. 2022. "Physical Properties of Extrudates With Fibrous Structures Made of Faba Bean Protein Ingredients Using High Moisture Extrusion." *Foods* 11, no. 9: 1280. https://doi.org/10.3390/foods11091280.

Kendler, C., A. Duchardt, H. P. Karbstein, and M. A. Emin. 2021. "Effect of Oil Content and Oil Addition Point on the Extrusion Processing of Wheat Gluten-Based Meat Analogues." *Foods* 10, no. 4: 697. https://doi.org/10.3390/foods10040697.

Koksel, F., and M. T. Masatcioglu. 2018. "Physical Properties of Puffed Yellow Pea Snacks Produced by Nitrogen Gas Assisted Extrusion Cooking." *LWT* 93: 592–598. https://doi.org/10.1016/j.lwt.2018.04.011.

Lemus-Conejo, A., F. Rivero-Pino, S. Montserrat-de la Paz, and M. C. Millan-Linares. 2023. "Nutritional Composition and Biological Activity of Narrow-Leafed Lupins (*Lupinus angustifolius* L.) Hydrolysates and Seeds." *Food Chemistry* 420: 136104. https://doi.org/10.1016/j.foodchem. 2023.136104.

Lin, S., H. E. Huff, and F. Hsieh. 2000. "Texture and Chemical Characteristics of Soy Protein Meat Analog Extruded at High Moisture." *Journal of Food Science* 65, no. 2: 264–269. https://doi.org/10.1111/j.1365-2621.2000. tb15991.x.

Ling, J. K. U., J. H. Sam, J. Jeevanandam, Y. S. Chan, and J. Nandong. 2022. "Thermal Degradation of Antioxidant Compounds: Effects of Parameters, Thermal Degradation Kinetics, and Formulation Strategies." *Food and Bioprocess Technology* 15, no. 9: 1919–1935. https://doi.org/10.1007/s11947-022-02797-1.

Lqari, H., J. Vioque, J. Pedroche, and F. Millán. 2002. "Lupinus angustifolius Protein Isolates: Chemical Composition, Functional Properties and Protein Characterization." Food Chemistry 76, no. 3: 349–356. https://doi.org/10.1016/S0308-8146(01)00285-0.

Luo, S., and F. Koksel. 2020. "Physical and Technofunctional Properties of Yellow Pea Flour and Bread Crumb Mixtures Processed With Low Moisture Extrusion Cooking." *Journal of Food Science* 85, no. 9: 2688–2698. https://doi.org/10.1111/1750-3841.15385.

Mazumder, K., B. Biswas, P. Kerr, et al. 2021. "Comparative Assessment of Nutritional, Thermal, Rheological and Functional Properties of Nine Australian Lupin Cultivars." *Scientific Reports* 11: 21515. https://doi.org/10.1038/s41598-021-00838-x.

Mohamad Mazlan, M., R. A. Talib, N. L. Chin, et al. 2020. "Physical and Microstructure Properties of Oyster Mushroom-Soy Protein Meat Analog via Single-Screw Extrusion." *Foods* 9, no. 8: 1023. https://doi.org/10.3390/foods9081023.

Monteiro, M. R. P., A. B. P. Costa, S. F. Campos, et al. 2014. "Evaluation of the chemical composition, protein quality and digestibility of lupin (Lupinus albus and Lupinus angustifolius)." *O Mundo da Saúde* 38: 251 – 259. https://api.semanticscholar.org/CorpusID:19528343.

Munteanu, I. G., and C. Apetrei. 2021. "Analytical Methods Used in Determining Antioxidant Activity: A Review." *International Journal of Molecular Sciences* 22, no. 7: 3380. https://doi.org/10.3390/ijms22073380.

Naumann, S., U. Schweiggert-Weisz, A. Martin, M. Schuster, and P. Eisner. 2021. "Effects of Extrusion Processing on the Physiochemical and Functional Properties of Lupin Kernel Fibre." *Food Hydrocolloids* 111: 106222. https://doi.org/10.1016/j.foodhyd.2020.106222.

Olt, V., J. Báez, R. Curbelo, et al. 2023. "Tannat Grape Pomace as an Ingredient for Potential Functional Biscuits: Bioactive Compound Identification, in Vitro Bioactivity, Food Safety, and Sensory Evaluation." Frontiers in Nutrition 10: 1241105. https://doi.org/10.3389/fnut.2023. 1241105.

Ortiz, D., A. Ponrajan, J. P. Bonnet, T. Rocheford, and M. G. Ferruzzi. 2018. "Carotenoid Stability During Dry Milling, Storage, and Extrusion Processing of Biofortified Maize Genotypes." *Journal of Agricultural and Food Chemistry* 66, no. 18: 4683–4691. https://doi.org/10.1021/acs.jafc. 7b05706

Osen, R., S. Toelstede, F. Wild, P. Eisner, and U. Schweiggert-Weisz. 2014. "High Moisture Extrusion Cooking of Pea Protein Isolates: Raw Material Characteristics, Extruder Responses, and Texture Properties." *Journal of Food Engineering* 127: 67–74. https://doi.org/10.1016/j.jfoodeng.2013.11. 023.

Öztürk, Z., M. Lille, N. Rosa-Sibakov, and N. Sozer. 2024. "Impact of Heat Treatment and High Moisture Extrusion on the In vitro Protein Digestibility of Sunflower and Pea Protein Ingredients." *LWT* 214: 117133. https://doi.org/10.1016/j.lwt.2024.117133.

Palanisamy, M., K. Franke, R. G. Berger, V. Heinz, and S. Töpfl. 2019. "High Moisture Extrusion of Lupin Protein: Influence of Extrusion Parameters on Extruder Responses and Product Properties." *Journal of the Science of Food and Agriculture* 99, no. 5: 2175–2185. https://doi.org/10.1002/jsfa.9410.

Pang, J., E. Guan, Y. Yang, M. Li, and K. Bian. 2021. "Effects of Wheat Flour Particle Size on Flour Physicochemical Properties and Steamed Bread Quality." *Food Science & Nutrition* 9, no. 9: 4691–4700. https://doi.org/10.1002/fsn3.2008.

Pasarin, D., V. Lavric, C. E. Enascuta, A.-I. Ghizdareanu, and C. B. Matei. 2023. "Optimal Enzymatic Hydrolysis of Sweet Lupine Protein Towards Food Ingredients." *Fermentation* 9, no. 3: 203. https://doi.org/10.3390/fermentation9030203.

Patil, S., S. K. Sonawane, M. Mali, S. T. Mhaske, and S. S. Arya. 2020. "Pasting, Viscoelastic and Rheological Characterization of Gluten Free (cereals, legume and underutilized) Flours With Reference to Wheat Flour." *Journal of Food Science and Technology* 57, no. 8: 2960–2966. https://doi.org/10.1007/s13197-020-04328-2.

Pietsch, V. L., J. M. Bühler, H. P. Karbstein, and M. A. Emin. 2019. "High Moisture Extrusion of Soy Protein Concentrate: Influence of Thermomechanical Treatment on Protein-Protein Interactions and Rheological Properties." *Journal of Food Engineering* 251: 11–18. https://doi.org/10.1016/j.jfoodeng.2019.01.001.

Plattner, B. J., S. Hong, Y. Li, et al. 2024. "Use of Pea Proteins in High-Moisture Meat Analogs: Physicochemical Properties of Raw Formulations and Their Texturization Using Extrusion." *Foods* 13, *no.* 8: 1195. https://doi.org/10.3390/foods13081195.

Rajendra, A., D. Ying, R. D. Warner, M. Ha, and Z. Fang. 2023. "Effect of Extrusion on the Functional, Textural and Colour Characteristics of Texturized Hempseed Protein." *Food and Bioprocess Technology* 16, no. 1: 98–110. https://doi.org/10.1007/s11947-022-02923-z.

Ramos-Diaz, J. M., S. Oksanen, K. Kantanen, et al. 2023. "Characterization of Texturized Meat Analogues Containing Native Lupin Flour and Lupin Protein Concentrate/Isolate." *Heliyon* 9, no. 10: e20503. https://doi.org/10.1016/j.heliyon.2023.e20503.

Rapinski, M., R. Raymond, D. Davy, et al. 2023. "Local Food Systems Under Global Influence: The Case of Food, Health and Environment in Five Socio-Ecosystems." *Sustainability* 15, no. 3: 2376. https://doi.org/10.3390/su15032376.

Rodríguez Arzuaga, M., A. G. Abraham, L. Suescun, et al. 2024. "Storage Stability of Model Infant Formula Powders Produced Under Varying Wet-mix Processing Conditions." *International Dairy Journal* 155: 105968. https://doi.org/10.1016/j.idairyj.2024.105968.

Roman, L., E. Tsochatzis, K. Tarin, E. M. Röndahl, C.-O. Ottosen, and M. Corredig. 2023. "Compositional Attributes of Blue Lupin (Lupinus angustifolius) Seeds for Selection of High-Protein Cultivars." *Journal of Agricultural and Food Chemistry* 71, no. 45: 17308–17320. https://doi.org/10.1021/acs.jafc.3c04804.

Ruiz-Gutiérrez, M. G., C. A. Amaya-Guerra, A. Quintero-Ramos, et al. 2015. "Effect of Extrusion Cooking on Bioactive Compounds in Encapsulated Red Cactus Pear Powder." *Molecules (Basel, Switzerland)* 20, no. 5: 8875–8892. https://doi.org/10.3390/molecules20058875.

Saldanha do Carmo, C., S. H. Knutsen, G. Malizia, et al. 2021. "Meat Analogues From a Faba Bean Concentrate Can be Generated by High Moisture Extrusion." *Future Foods* 3: 100014. https://doi.org/10.1016/j.fufo.2021.100014.

Schmid, E. M., A. Farahnaky, B. Adhikari, and P. J. Torley. 2022. "High Moisture Extrusion Cooking of Meat Analogs: A Review of Mechanisms of Protein Texturization." *Comprehensive Reviews in Food Science and Food Safety* 21, no. 6: 4573–4609. https://doi.org/10.1111/1541-4337.13030.

Schreuders, F. K. G., M. Schlangen, I. Bodnár, P. Erni, R. M. Boom, and A. J. van der Goot. 2022. "Structure Formation and Non-Linear Rheology of Blends of Plant Proteins With Pectin and Cellulose." *Food Hydrocolloids* 124: 107327. https://doi.org/10.1016/j.foodhyd.2021.107327.

Schreuders, F. K. G., B. L. Dekkers, I. Bodnár, P. Erni, R. M. Boom, and A. J. van der Goot. 2019. "Comparing Structuring Potential of Pea and Soy Protein with Gluten for Meat Analogue Preparation." *Journal of Food Engineering* 261: 32–39. https://doi.org/10.1016/j.jfoodeng.2019.04.022.

Seregina, I. I., O. G. Volobueva, V. I. Trukhachev, S. L. Belopukhov, I. I. Dmitrevskaya, and A. V. Zhevnerov. 2024. "Morphological and Physiological Properties of Lupine Nodule Bacteria (*Bradyrhizobium lupini*) When Grown on a Typical Urban Soil." *Brazilian Journal of Biology* 84: e277549. https://doi.org/10.1590/1519-6984.277549.

Sha, L., and Y. L. Xiong. 2020. "Plant Protein-Based Alternatives of Reconstructed Meat: Science, Technology, and Challenges." *Trends in Food Science and Technology* 102: 51–61. https://doi.org/10.1016/j.tifs.2020. 05.022.

- Shan, S., C. Teng, D. Chen, and O. Campanella. 2023. "Insights Into Protein Digestion in Plant-Based Meat Analogs." *Current Opinion in Food Science* 52: 101043. https://doi.org/10.1016/j.cofs.2023.101043.
- Singh, A., M. C. Tulbek, M. Izydorczyk, and F. Koksel. 2025. "High Moisture Extrusion Texturization of Air-Classified Barley Protein for the Production of Novel Plant-Based Meat Analogues." *Food and Bioprocess Technology* 18, no. 2: 1857–1872. https://doi.org/10.1007/s11947-024-03549-z.
- Singh, R., A. G. A. Sá, S. Sharma, et al. 2024. "Effects of Feed Moisture Content on the Physical and Nutritional Quality Attributes of Sunflower Meal-Based High-Moisture Meat Analogues." *Food and Bioprocess Technology* 17, no. 7: 1897–1913. https://doi.org/10.1007/s11947-023-03225-8.
- Singh, R., and F. Koksel. 2021. "Effects of Particle Size Distribution and Processing Conditions on the Techno-Functional Properties of Extruded Soybean Meal." *LWT* 152: 112321. https://doi.org/10.1016/j.lwt.2021.112321.
- Sujak, A., A. Kotlarz, and W. Strobel. 2006. "Compositional and Nutritional Evaluation of Several Lupin Seeds." *Food Chemistry* 98, no. 4: 711–719. https://doi.org/10.1016/j.foodchem.2005.06.036.
- UNDP. n.d. "Sustainable Development Goals." Retrieved July 12, 2024. https://www.undp.org/sustainable-development-goals.
- van der Sman, R. G. M., and A. J. van der Goot. 2023. "Hypotheses Concerning Structuring of Extruded Meat Analogs." *Current Research in Food Science* 6: 100510. https://doi.org/10.1016/j.crfs.2023.100510.
- Villarino, C. B. J., V. Jayasena, R. Coorey, S. Chakrabarti-Bell, and S. K. Johnson. 2016. "Nutritional, Health, and Technological Functionality of Lupin Flour Addition to Bread and Other Baked Products: Benefits and Challenges." *Critical Reviews in Food Science and Nutrition* 56, no. 5: 835–857. https://doi.org/10.1080/10408398.2013.814044.
- Wang, X., Z. He, M. Zeng, F. Qin, B. Adhikari, and J. Chen. 2017. "Effects of the Size and Content of Protein Aggregates on the Rheological and Structural Properties of Soy Protein Isolate Emulsion Gels Induced by CaSO4." *Food Chemistry* 221: 130–138. https://doi.org/10.1016/j.foodchem. 2016.10.019.
- Wi, G., J. Bae, H. Kim, Y. Cho, and M.-J. Choi. 2020. "Evaluation of the Physicochemical and Structural Properties and the Sensory Characteristics of Meat Analogues Prepared With Various Non-Animal Based Liquid Additives." *Foods* 9, no. 4: 461. https://doi.org/10.3390/foods9040461.
- Yang, F., X. Liu, X. Ren, Y. Huang, C. Huang, and K. Zhang. 2018. "Swirling Cavitation Improves the Emulsifying Properties of Commercial Soy Protein Isolate." *Ultrasonics Sonochemistry* 42: 471–481. https://doi.org/10.1016/j.ultsonch.2017.12.014.
- Yang, G., Y. Bao, K. Sun, C. Chang, and W. Liu. 2020. "Effects of Covalent Interactions and Gel Characteristics on Soy Protein-tannic Acid Conjugates Prepared Under Alkaline Conditions." *Food Hydrocolloids* 112: 106293. https://doi.org/10.1016/j.foodhyd.2020.106293.
- Zahari, I., F. Ferawati, A. Helstad, et al. 2020. "Development of High-Moisture Meat Analogues With Hemp and Soy Protein Using Extrusion Cooking." *Foods* 9, no. 6: 772. https://doi.org/10.3390/foods9060772.
- Zahari, I., S. Rinaldi, C. Ahlstrom, K. Östbring, M. Rayner, and J. Purhagen. 2023. "High Moisture Meat Analogues From Hemp—The Effect of Co-Extrusion With Wheat Gluten and Chickpea Proteins on the Textural Properties and Sensorial Attributes." *LWT* 189: 115494. https://doi.org/10.1016/j.lwt.2023.115494.
- Zhang, T., J. Guo, J.-F. Chen, J.-M. Wang, Z.-L. Wan, and X.-Q. Yang. 2020. "Heat Stability and Rheological Properties of Concentrated Soy Protein/Egg White Protein Composite Microparticle Dispersions." *Food Hydrocolloids* 100: 105449. https://doi.org/10.1016/j.foodhyd.2019.105449.
- Zhang, Y., R. Brouwer, G. Sala, E. Scholten, and M. Stieger. 2024. "Exploring Relationships Between Juiciness Perception, Food and Bolus Properties of Plant-Based Meat Analogue and Beef Patties." *Food Hydrocolloids* 147: 109443. https://doi.org/10.1016/j.foodhyd.2023.109443.

- Zhang, Z., and Y. Liu. 2017. "Recent Progresses of Understanding the Viscosity of Concentrated Protein Solutions." *Current Opinion in Chemical Engineering* 16: 48–55. https://doi.org/10.1016/j.coche.2017.04.001.
- Zheng, J., S. Huang, R. Zhao, N. Wang, J. Kan, and F. Zhang. 2021. "Effect of Four Viscous Soluble Dietary Fibers on the Physicochemical, Structural Properties, and in Vitro Digestibility of Rice Starch: A Comparison Study." *Food Chemistry* 362: 130181. https://doi.org/10.1016/j.foodchem. 2021.130181.

Supporting Information

Additional supporting information can be found online in the Supporting Information section.

 $\label{eq:Supporting Fig.1V} Supporting Fig.1V is cosity profiles as a function of time during heating of different formulations based on soy protein isolate (SPI), lupin flour (LF), and lupin protein concentrate (LPC), along with the corresponding temperature evolution (grey line). (A) Formulations with SPI/LF (B) Formulations containing LPC and LF/SPI.$